SAPIENZA
UNIVERSITÀ DI ROMA

Dottorato di ricerca Neuroscienze clinico/sperimentali e Psichiatria

XXXI ciclo

A.A. 2017/2018

"Ca^{2+}-activated K^{+}channels modulate microglia affecting motor neuron survival in $hSOD1^{G93A}$ mice"

PhD student

Germana Cocozza

Tutor

Prof. Cristina Limatola

Coordinator

Prof. Marco Salvetti

INDEX

OVERVIEW

Amyotrophic lateral sclerosis (ALS) is a multifactorial disease characterized by the progressive degeneration of motor neurons (MN) and muscle paralysis. Despite current treatments, patients survive less than 3–5 years after the initial diagnosis. Most ALS cases are sporadic (sALS), and only 5-10% have a familial origin (fALS). Among the latter, about 20% express a dominant mutant form of the Cu, Zn superoxide dismutase (SOD1) (Rothstein, 2009). Transgenic mice expressing a mutant SOD1 develop MN pathology, with muscle denervation and weakness similar to ALS patients (Fischer et al., 2004). Many evidence demonstrate that ALS is non-cell autonomous, with multiple co-players involved in disease progression (Robberecht et al, 2013). In particular, signals from both glial cells and muscles initiate and sustain MN degeneration (Boillée et al., 2006; Dobrowolny et al, 2008). Recent studies described a critical role for microglia in amyotrophic lateral sclerosis (ALS), where these CNS-resident immune cells participate in the establishment of an inflammatory microenvironment that contributes to motor neuron degeneration. Understanding the mechanisms leading to microglia activation in ALS could help to identify specific molecular pathways which could be targeted to reduce or delay motor neuron degeneration and muscle paralysis in patients. The intermediate-conductance calcium-activated potassium channel KCa3.1 has been reported to modulate the "pro-inflammatory" phenotype of microglia in different pathological conditions. We here investigated the effects of blocking KCa3.1 activity in the hSOD1^{G93A}ALS mouse model, which recapitulates many features of the human disease. We report that treatment of hSOD1^{G93A} mice with a selective KCa3.1 inhibitor, 1-[(2-chlorophenyl) diphenylmethyl]-1*H*-pyrazole (TRAM-34), attenuates the "pro-inflammatory" phenotype of microglia in the spinal cord, reduces motor neuron death, delays onset of muscle weakness, and increases survival. Specifically, inhibition of KCa3.1 channels slowed muscle denervation, decreased the expression of the fetal acetylcholine receptor γ subunit and reduced neuromuscular junction damage. Taken together, these results demonstrate a key role for KCa3.1 in driving a pro-inflammatory microglia phenotype in ALS.

INTRODUCTION

1. Amyotrophic Lateral Sclerosis (ALS)

Amyotrophic lateral sclerosis (ALS) is a fatal, adult-onset neurodegenerative disease that is characterized by the degeneration of both upper motor neurons (that is, neurons that project from the cortex to the brainstem and the spinal cord) and lower motor neurons (that is, neurons that project from the brainstem or spinal cord to muscle), leading to paralysis and death of the patient in mean 3–5 years after the onset of disease.

1.1 Introduction/Background

The earliest cases of ALS were probably described by Aran (1848)[1] and Cruveilhier (1853)[2] although it was not until 1869 that the specific entity we now recognize as ALS was formally defined and identified by Charcot[3]. Its name reflects both the degeneration of corticospinal motor neurons, the descending axons of which in the lateral spinal cord seem scarred (lateral sclerosis), and the demise of spinal motor neurons, with secondary denervation and muscle wasting (amyotrophy). ALS is known as Lou Gehrig's disease in the United States and as motor neuron disease in the United Kingdom. Traditionally, ALS has been classified as either the sporadic or familial form. About 10% of cases are considered "familial ALS" (FALS) and five major genes are currently associated with familial ALS (C9orf72, SOD1, FUS, TARDBP and TBK1)[4,5,6]. The SOD1 gene was the first associated with ALS and most ALS mouse models currently used are based upon overexpression of mutant forms of SOD1[7]. Primary symptoms begin as mild cramps or weakness in the limbs or bulbar muscles which then progress to paralysis of almost all skeletal muscles. Some subsets of motor neurons, including those that innervate the extraocular muscles or sphincters, are spared until late in the progression of the disease. Beyond motor symptoms, up to 50% ALS patients develop cognitive and/or behavioral impairment during the course of disease, and 13% of patients have cognitive abnormalities common to frontotemporal dementia (FTD)[8]. Protein aggregates of hexanucleotide repeat expansion in C9orf72 (encoding guanine nucleotide exchange C9orf72) have been detected in both ALS and frontotemporal dementia patients[9].

1.2 Epidemiology

Most population-based epidemiological studies of ALS have been combined to form the European ALS Epidemiology Consortium (EURALS), which has provided data comparing the incidence of ALS between European countries. According to the latest studies, the incidence of ALS varies according to ancestral origin; studies in populations of European origin have shown a greater incidence (2.6-3.0 cases per 100,000 individuals[10]) than in East Asia (~ 0.8 cases per 100,000 individuals) and in South Asia (~ 0.7 cases per 100,000 individuals). In some regions (such as Guam and the Kii peninsula in Japan) the reported incidence was very high but has decreased substantially in the last 30 years for reasons that are not clear. Evidence suggests that the incidence and prevalence of ALS is lower in populations of mixed ancestral origin than in European populations, with differences in age of onset in genetically heterogeneous populations. In populations of European ancestry, the median age of onset of sporadic ALS is 65 years, whereas in genetically heterogeneous populations is about 10 years earlier [11]. In most population-based studies, ALS is found to be more common in men than in women, affecting 1.2–1.5 men for every woman[12]. In Europe, most men have spinal-onset disease, and women have a higher propensity for bulbar-onset diseas[11]. The main limitation of the global epidemiology of ALS is that about 80% of studies have been conducted in Europe and the United States. The risk of developing ALS peaks peaks between 50–75 years of age and decreases thereafter, compared to Alzheimer's disease. Survival is highly variable, but respiratory failure usually leads to death about 3–4 years after onset[13]. In the future, it will be necessary to deepen the researches to understand the roles of ancestry, genetics and environmental exposure in the causality of ALS.

1.3 Mechanisms and pathophysiology

Autopsies of people with ALS reveal the degeneration of motor neurons in the motor cortex of the brain, in the brainstem motor nuclei and in the anterior horns of the spinal cord and diffuse astrocytic gliosis and microglial infiltration in the gray and white matter of the spinal cord. Skeletal muscle shows features of denervation and reinnervation, with fiber type grouping and clusters of angular atrophic fibers. Although the fundamental pathophysiological mechanisms underlying ALS are not yet well known, the neuropathological sign of the disease is the aggregation and accumulation of ubiquitous protein inclusions in motor neurons. Other pathological features are associated with specific

genes. For example, cases of ALS caused by a large expansion of a hexanucleotide repeat in C9orf72[14] as well as neuronal cytoplasmic inclusions containing the protein DNA binding protein 43 (TDP-43), encoded by the TARDBP gene, which is the main component of ubiquitous inclusions in most cases of ALS[15]. Or again, cases of ALS caused by mutations in the SOD1 or FUS genes show abnormal SOD1 or FUS protein inclusions, respectively (table 1, from *Hardiman et al., Nature Reviews Disease Primers, 2017*). In addition to these alterations in motor neurons, there is also abundant evidence of relevant pathology in non-neural cell types (eg, astrogliosis and microgliosis) that could negatively influence disease progression. A very important discovery was the identification of dominant mutations in the SOD1 gene, which encodes a abundant and ubiquitous cytoplasmic enzyme called Cu-Zn superoxide dismutase[7,17,18], an important antioxidant.

Table 1 | **Main genes implicated in amyotrophic lateral sclerosis**

Locus	Gene (protein)	Inheritance	Implicated disease mechanisms	Refs
ALS1	*SOD1* (superoxide dismutase 1)	AD or AR	Oxidative stress	234,235
ALS2	*ALS2* (alsin)	AR	Endosomal trafficking	236,237
ALS3	Unknown	AD	Unknown	238
ALS4	*SETX* (senataxin)	AD	RNA metabolism	239
ALS5	Unknown	AR	DNA damage repair and axon growth	240
ALS6	*FUS* (RNA-binding protein FUS)	AD or AR	RNA metabolism	241,242
ALS7	Unknown	AD	Unknown	243
ALS8	*VAPB* (vesicle-associated membrane protein-associated protein B/C)	AD	Endoplasmic reticulum stress	42
ALS9	*ANG* (angiogenin)	AD	RNA metabolism	244
ALS10	*TARDBP* (TAR DNA-binding protein 43)	AD	RNA metabolism	27,245
ALS11	*FIG4* (polyphosphoinositide phosphatase)	AD	Endosomal trafficking	246
ALS12	*OPTN* (optineurin)	AD or AR	Autophagy	247
ALS13	*ATXN2* (ataxin 2)	AD	RNA metabolism	248
ALS14	*VCP* (valosin-containing protein)	AD	Autophagy	36
ALS15	*UBQLN2* (ubiquilin-2)	XD	UPS and autophagy	34
ALS16	*SIGMAR1* (sigma non-opioid intracellular receptor 1)	AD	UPS and autophagy	249,250
ALS17	*CHMP2B* (charged multivesicular body protein 2B)	AD	Endosomal trafficking	251
ALS18	*PFN1* (profilin 1)	AD	Cytoskeleton	97
ALS19	*ERBB4* (receptor tyrosine-protein kinase erbB 4)	AD	Neuronal development	252
ALS20	*HNRNPA1* (heterogeneous nuclear ribonucleoprotein A1)	AD	RNA metabolism	82
ALS21	*MATR3* (matrin 3)	AD	RNA metabolism	83
ALS22	*TUBA4A* (tubulin α4A)	AD	Cytoskeleton	102
ALS-FTD1	*C9orf72* (guanine nucleotide exchange C9orf72)	AD	RNA metabolism and autophagy	5,6
ALS-FTD2	*CHCHD10* (coiled-coil-helix-coiled-coil-helix domain-containing 10)	AD	Mitochondrial maintenance	253
ALS-FTD3	*SQSTM1* (sequestosome 1)	AD	Autophagy	254
ALS-FTD4	*TBK1* (serine/threonine-protein kinase TBK1)	Unknown	Autophagy	53,54

AD, autosomal dominant; AR, autosomal recessive; UPS, ubiquitin–proteasome system; XD, X-linked dominant

Hardiman et al., Nature Reviews Disease Primers, 2017

The normal function of SOD1 is to catalyze the conversion of highly reactive superoxide to hydrogen peroxide or oxygen. The expression of the mutant SOD1 in mice demonstrated that motor neuron degeneration is determined by one or more acquired toxicities of the

mutant protein and is independent of the activity of dismutase[19,20,21]. The gene mutations that cause ALS are expressed in many types of cells and this means that the disease is the result of a combination of SOD1 mutant damage both in motoneurons and in their glial partners, rather than damage to neurons alone. It is now clear that ALS acts through non cell-autonomous mechanisms. For example, studies in mice expressing mutated SOD1 reveal that high levels of expression in all motor neurons are not sufficient to cause early-onset disease[19]. In contrast, a reduction in the synthesis of the mutant SOD1 in motoneurones does not slow down the rate of progression after the onset of the disease, even if applied before the symptoms occur[22,23].

Therefore, ALS is a disease not only of the motor neuron but also of the motor system, which is composed of motor neurons and intimately associated cells of different types. Great progress has been made with the development of pathology models in rats, mice, zebrafish, flies, worms and yeasts to study how mutations cause motor neuron degeneration and to modulate the biological processes that are thought to be important in disease pathology. Obviously, these models have limitations and none recapitulates completely human disease. The main reason is that all these models are based on gene overexpression (with multiple copies of the human variant inserted in the transgenic model) and because human neurotransmission differs substantially from that of the lower animals. In ALS, different pathophysiological mechanisms are implicated in motor neuronal damage, although these mechanisms are often interconnected. SOD1 is the longest studied gene implicated in ALS and has been linked to the greatest number of pathophysiological mechanisms. Aberrant RNA metabolism[24,25]and altered protein homeostasis[26] are predominant factors that link multiple causal ALS genes to neuronal damage. Mitochondrial dysfunction can result from a mutation in CHCHD10 and secondary respiratory chain deficiencies that result from protein aggregates generated in the presence of other ALS-associated mutations[27]. Both cases lead to an increase in oxidative stress, which places additional stress on an already compromised protein homeostasis system. Other mechanisms of ALS can directly alter neuronal function (such as alteration of nuclear export, altered DNA repair and transport of dysregulated vesicle) and dysfunction of glial cells[28,29]. Furthermore, neuronal hyperexcitability[30,31] and axon dysfunction have been implicated in ALS[32]. Each of these factors contributes to the general pathology of the human disease, but it would be wrong to think that all these factors are involved in all cases of ALS, since the human disease is heterogeneous. Nevertheless, they represent our current knowledge base on the pathophysiology of ALS and are the starting point for current and future therapeutic initiatives.

1.4 Diagnosis, screening and therapies

Diagnosing ALS is based on the El Escorial and Airlie House criteria[33-34]. Diagnosis according to these criteria is used for patients who have a history of progressive weakness spreading within a region or to other regions (bulbar, cervical, thoracic, or lumbar), with evidence of the involvement of lower motor neurons (through the presence of specific symptoms or evidence of denervation on electromyography) and upper motor neurons (clinical). Genetic testing can also be included in patients with a family history of ALS[35] and clinical evidence of disease, although this is not uniformly applied across centres[36]. The heterogeneous clinical presentation and varying speed of progression make diagnosis of ALS challenging. Several biochemical prognosis markers have been reported, including serum urate, serum creatinine, serum chloride and increased serum neurofilament levels and in CSF[37]. The worsening of respiratory function, assessed by measuring slow vital capacity, forced vital capacity and nasal inspiratory pressure, is also related to short survival[38,39,40]. MRI studies have reported corticospinal tract degeneration, with extensive involvement of the frontal and temporal regions and basal ganglia in patients with ALS, compared with controls. Furthermore, these analyses are also supported by studies using spectral electroencephalography[41] and findings that patients with different degrees of cognitive impairment have significantly different patterns of frontal lobe metabolic impairment when assessed using 18F–fluorodeoxyglucose PET imaging[42]. However, these types of tests can not provide individualized data that can be used as a reliable biomarker of upper motor neuron dysfunction or cognitive impairment in ALS patients. Weight loss is common in ALS and is multifactorial (muscle loss, hypermetabolism, difficulty eating [swallowing, shortness of breath] or decreased appetite)[43]. If weight loss is greater than 10% of body weight, the guidelines recommend that patients undergo gastrostomy to nurture and support feeding and medication[44]. Furthermore, non-invasive ventilation has been shown to prolong survival with a larger effect size than riluzole, but unfortunately it is not always feasible, particularly for patients with cognitive or bulbar impairment impairment[45]. However, the results of a large cohort study (n = 929)[46] suggest that non-invasive ventilation also improves survival in patients with bulbar onset, so all patients should be offered non-invasive ventilation, even when it is likely that the procedure is poorly tolerated.

Although over 50 drugs have been studied with different mechanisms of action for the treatment of ALS, only two compounds (riluzole and edaravone) have been approved. Riluzole was the first FDA-approved treatment for ALS and, the drug works by reducing

glutamatergic neurotransmission by blocking voltage-gated sodium channels on presynaptic neurons. Published data showed that riluzole increased 3-month survival after 18 months of treatment compared to placebo, but had no significant effect on muscle strength[47]. Riluzole is a relatively safe drug, although the most common adverse effects are an increase in liver enzymes and asthenia; and some cases of fatal hepatic failure and pancreatic arthritis have been reported[48]. Edaravone, which is believed to act as an antioxidant, may slow the progression of the disease in patients with early onset and rapidly progressing disease[49]; and it has been approved by the FDA but not by the European Medicines Agency[50]. In recent years the number of new treatments for ALS has increased considerably and some of these drugs are aimed at known mutations and pathogenetic pathways. Symptomatic therapies, including Tirasemtiv, are based on improving respiratory function in patients with ALS and are currently in Phase III; Phase I studies evaluating the use of antisense oligonucleotides in ALS related to SOD1[51] and C9orf72 are also ongoing[52].

2. Microglia

During the course of many diseases, microglial cells lose their homeostatic molecular signature and function and become chronically inflammatory.

2.1 Historical features

It was Pio del Rio-Hortega in 1932 that first introduced the concept of microglia in a book chapter called "Microglia"[53], even if these cells had already been identified in the early 20th century by Ramon y Cajal, that in 1913 described the "third elements" of SNC. In his article,del Rio-Hortega stated notions that nowadays have become postulates, such as: - microglia has mesodermal origin and enter the brain during early development; these invading cells use vessels and white matter tracts as guiding structures for migration and enter all brain regions; they can assume a branched, ramified morphology in the mature brain (known today as the resting microglia); after a pathological event, these cells undergo a transformation, that let them acquire an amoeboid morphology; these cells have the capacity to migrate, proliferate and phagocytize. Del Rio-Hortega called the newly discovered cell class microglia and the individual cell "microgliacyte". In 1939 Kershman introduced the classification of the three classical microglia phenotypes: ramified, intermediate, amoeboid. For many years the field did not advance beyond these statements. The modern era of microglia research started in the late 1960s whit Georg Kreutzberg. He studied microglia responses to injury in tissue with an intact blood-brain barrier. His work also provided the possibility to distinguish between responses of intrinsic microglia and invading monocytes and helped to establish the concept that microglia is important for regeneration of the brain. Nowadays with the introduction of microglial cultures, the research made many strides and we are very close to understand the real function of these immune cells, considered as residing macrophages (the innate immune cells that are a homologue of brain microglia), of CNS. The origin of microglia has now been clearly defined and shown to relate to the early colonization of the CNS by mesodermal progenitors that arise from the yolk sac[54,55,56]. It is now recognized that monocytes and tissue macrophages are not, as had been previously proposed, microglia progenitors in either health or disease and that, in adulthood, microglia are an independent self-renewing population[57,58,59]. Human microglia turn over at a yearly median rate of 28% and live, on average, for 4.2 years. Thus, most of the microglial population is renewed several times over

the course of a lifetime[60]. In support of the importance of microglial self-renewal, a recent study demonstrated that the repopulated microglia that rapidly replenish the adult brain's microglial population after microglial depletion are solely derived from the proliferation of residual microglia and not from newly generated progenitors[61].It has been recently shown that microglia expresses not only specific markers like Cx3cr1, CD11b, Iba1 and F4/80[62], but RNA-seq analysis identified a new set of microglia-specific markers in the healthy brain that include HexB, P2ry12, S100A8, S100A9, Tmem119, Gpr34, SiglecH, TREM2, and Olfml3[63].

2.2 Physiological functions of microglia

Microglia represent about 5-12% of total cells of CNS, being present throughout the brain, with different density and distribution[64]. Microglia functions are important at various stages of development from embryonic stages to adulthood and aging. These cells have three essential functions: (i) sense their environment, (ii) conduct physiological housekeeping, and (iii) protect against modified-self and non-self injurious agents. An important message is that there is no resting microglia. Their sensing, housekeeping, and protecting functions keep them constantly engaged, and most microglia in healthy brains are capable of performing such functions. Microglia studies have revealed that these cells have highly dynamic processes and continuously monitor their local environment[65,66]. It is estimated that the resident microglia can scan the entire brain parenchyma every few hours[67,68], suggesting that they have homeostatic functions in the healthy brain during which they actively contact other neural components, including synaptic clefts, with their fine processes. ATP is likely one of many signals that mediate microglia–neuron communication, and microglial processes are rapidly attracted to the source of ATP release[65]. Microglia play a crucial role in synaptogenesis, trophic support, chemotaxis and neurogenesis. In order to shape neuronal circuits during development, microglia mediate synaptic and axonal pruning by phagocytizing inappropriate synaptic connections and axons[69,70]. Microglia mediate synaptogenesis at prenatal stages[71], with the secretion of several factors, such as nerve growth factor (NGF), brain-derived neurotrophic factor (BDNF) and neurotrophin 3 (NT3), and also these cells promote learning- dependent synapse formation through the secretion of BDNF in mice[72]. It also been shown that microglia attract monocytes to the brain in a CC-chemokine ligand 2 (CCL2)-dependent fashion. These monocytes play an important role in

neuroinflammation. For example, in the SOD1 mice model of ALS, spinal microglia has been shown to recruit splenic monocytes expressing the CC-chemokine 2 receptor (CCR2) and high levels of 6C lymphocyte antigen (LY6C)[73]. In addition, microglial cells promote neurogenesis through phagocytosis of excessive neonate cells and through cytokine secretion. Most newly born cells in the developing nervous system undergo apoptotic death as they pass from neural progenitors to neuroblasts and are rapidly eliminated by microglia-mediated phagocytosis[74]. In addition, during neurogenesis in the adult hippocampus, microglia act through apoptosis-coupled phagocytosis.

2.3 Microglia in health and disease

It is now accepted that, during the course of many diseases, dysregulation of microglia functions results in an imbalance that initiates or propagates neurodegeneration and these cells become chronically inflammatory. Infection, trauma, ischemia, neurodegenerative diseases, glioma or any disturbance or loss of brain homeostasis evoke rapid and radical changes in microglial cell shape, gene expression and, in general, in the functional behavior defined as “microglial activation”. Mature microglia have highly ramified processes, whereas during development, they adopt an ‘amoeboid’ morphology with larger, rounder cell bodies and shorter, thicker branches. These morphological features during development are accompanied by higher levels of phagocytic activity as well as by distinct gene expression and secretory profiles. Microglia exhibit both phenotypic and functional plasticity in healthy and diseased brains[75-78]. In peripheral macrophages, cell phenotypes have been determined by the varied expression of cell surface receptors by these cells[79]. Similarly to macrophages, microglial phenotypes were characterized by the presence of particular cell surface molecules and the expression of specific sets of cytokines and were classified as either M1-like (exhibiting pro-inflammatory signaling and neurotoxicity) or M2-like (participating in the resolution of inflammation)[80]. However, it is now clear that this simplistic view of microglial phenotypes does not adequately describe the complex physiology of microglial cells[81]. The characterization of microglial diversity has therefore been redefined with the help of newly developed technologies, including RNA-sequencing, quantitative proteomics and epigenetic studies. Microglial activation may start with an early emergency response, such as defense-oriented functions, to fight off an infection or to limit further damage after an injury. The activated population with an initially chosen program may eventually convert to repair-oriented support for tissue restoration. When discussing the

acquisition of different phenotypes, the functional heterogeneity of microglia has to be considered, too. Regional heterogeneity and segregation of specific microglia population in tissues and preparations were demonstrated by morphology, selective detection of constitutive or inducible mRNAs and proteins. Heterogeneity was also observed in microglia from the aging brain where surprising differences between individuals were found[82,83]. These differences could impact on development, normal functionality, as well as vulnerability to inflammation[84]. Reactive gliosis and neuroinflammation are hallmarks of several neurodegenerative diseases, such as Alzheimer's disease (AD), Parkinson's disease (PD), amyotrophic lateral sclerosis (ALS), and frontal temporal dementia (FTD).

3. Microglia in ALS

Microglia is one of the most important populations involved in Amyotrophic lateral, where signals from these CNS-resident immune cells initiate and sustain MN degeneration.

3.1 Microglia: between neuroprotection and neurotoxicity

Autopsies[85] and PET imaging[86] in the brains of live ALS patients have shown microglia expressing proinflammatory markers at sites of motor neuron injury. Genes that are commonly mutated in ALS include superoxide dismutase 1 (SOD1), C9orf72 and TAR DNA-binding protein (TARDBP)[87]. Cytoplasmic aggregation by mutated genes in neurons and glia of ALS patients, and release of the accumulated cytoplasmic mutant SOD1 (mSOD1) to the extracellular space that can be taken up by other cells are common features[88,89]. Transgenic mice overexpressing human mutant *SOD1 (mSOD)* develop a progressive motor neuron disease similar to ALS[7,90]. In this transgenic model of familial ALS, some proinflammatory microglia are seen in the spinal cord before clinical disease develops, increase with disease progression, and persist into end-stage disease[91]. Yamanaka et al.,[92] have shown how the expression of mSOD1 specific in microglia accelerates disease onset and a few years later Apolloni et al.,[93] have shown how microglial activation contributes to neuronal death. Studies investigating the progression of the disease in ALS mice indicate that resident microglia also increase their number during disease progression[94]. In the early stages of the disease, microglia release neuroprotective molecules to prevent and contain neuronal degeneration. In particular, a trophic role for activated microglia has been suggested at early stages of the disease[95]. In the SOD1G93A mice, it was observed a decrease in microglia number in the entire SC at the pre-symptomatic age[96]. But with the disease progression, it has been shown that they become harmful, releasing neurotoxic factors NF-κ B-dependent[97] and partly mediated by IL-1β[98]. Several studies have also provided information on the mechanisms driving the changes in microglial signature in ALS. ALS is associated with neuronal death and the activation of TREM2–ApoE signaling in microglia by apoptotic neurons. This signaling activates miR-155, which has been shown to be a pro-inflammatory signal. In fact, the genetic deletion of Apoe abrogated the induction of miR-155 in microglia and increased survival in SOD1 mice[99]. Given that many of the microglial changes observed in ALS were also observed in a mouse model of AD, it is assumed that there exists a microglial response common to different pathological processes.

Transgenic mice carrying the human *C9orf72* gene, a hexanucleotide repeat expansion that is associated with ALS and frontotemporal dementia, show pathological features of ALS, without behavioral abnormalities or neurodegeneration[100]. Recent studies have shown in mice deficient in C9orf72, that microglia were strongly activated in the mutant with a higher production of TNF and IL-1 and defective maturation of phagosomes to lysosomes[101]. Further studies have shown that C9orf72 is required for normal microglial function and that impairment of capacity microglial elimination of the aggregated proteins by altering the maturation of phagosomes to lysosomes, an important step in the defense of the host, can contribute to neurodegeneration in patients with the C9orf72 expansion. Transgenic mice expressing inducible human *TDP-43 (hTDP43)* show a progressive loss of motor neurons but only slight microglial changes[102]. Unexpectedly, TARDBP was also found to regulate microglial phagocytosis. Following the suppression of the hTDP-43 transgene expression, microglia selectively eliminated the existing neuronal hTDP-43. When microgliosis was blocked during the early recovery phase using a CSF1R and c-Kit inhibitor, these mice failed to recover full motor function, suggesting a neuroprotective role for microglia. Interestingly, the conditional deletion of TDP43 in microglia led to increased β-amyloid clearance and leads to a greater loss of synapses[103], this could partially explain the less frequent occurrence of Alzheimer disease among patients with ALS. These studies demonstrated non-cell-autonomous pathology of ALS and raised the possibility of targeting microglia for treating neurodegenerative diseases.

4. Intermediate Conductance Calcium-Activated Potassium Channels (KCa3.1)

In the CNS, KCa3.1 channels are expressed by microglial cells, where they regulate cell migration and phagocytic activity in physiological and pathological conditions.

4.1 Calcium-activated potassium channels: properties

Ion channels are involved in several physiological and pathological cellular functions, and in hallmarks of cancer cell aggressiveness, such as proliferation and migration. In most cases, their contribution consists in regulating two important cellular parameters, the cell volume and the intracellular Ca^{2+} concentration ($[Ca^{2+}]i$)[104,105]. Modulation of these two parameters, in addition to the ClC-3 channels, requires the activity of Ca^{2+}-activated K-selective BK channels, often markedly upregulated in glioblastoma cells[106,107]. Ca^{2+} influx through the TRPC family of Ca^{2+}-permeable channels has indeed been shown to modulate glioblastoma cell cycle progression[108] and to induce a Ca^{2+}/calmodulin-dependent protein kinase II (CaMKII)-dependent activation of ClC-3 during premitotic volume condensation[109]. In addition, glioblastoma cell migration has been shown to be accompanied by intracellular Ca^{2+} oscillations that are instrumental to promote the kinase-dependent detachment of focal adhesions during cell rear retraction[110] and these intracellular Ca^{2+} oscillations can be significantly affected by the membrane hyper-polarization determined by the activity of K^+ channels[111].Ca^{2+}-activated K^+ (KCa) channels are at the crossroad where Ca^{2+} influx, membrane potential, and outward ion fluxes, integrate to modulate a large array of cellular processes[112]. The human genome contains eight KCa channels, which can be divided into two groups depending on their genetic relationship, their single channel conductance and the molecular mechanism of their Ca^{2+} sensitivity[113]. The first group encompasses KCa1.1, KCa4.1, KCa4.2 and KCa5.1, which were initially grouped together based on structural similarity but later found to differ in their activation mode. While the founding member of the group, KCa1.1, is indeed a true KCa channel and is activated by Ca^{2+} binding to a negatively charged segment in the C-terminus, KCa4 and KCa5 channels are activated by Na^+, Cl^- or alkalization[113]. The second group consists of the three small-conductance channels, KCa2.1 (SK1), KCa2.2 (SK2) and KCa2.3 (SK3), and the intermediate-conductance channel KCa3.1 (IK1, SK4) (Figure 1)[121]. KCa3.1 was cloned by three independent groups in 1997[114,115] and has approximately 42-44% sequence identity to the KCa2 channels. Like the KCa2 channels, KCa3.1 is voltage independent and is activated by

350 nM intracellular Ca^{2+} binding to the EF-hands of calmodulin, which is constitutively associated with the C-terminal region and serves as its Ca^{2+}-sensing-subunit[116].

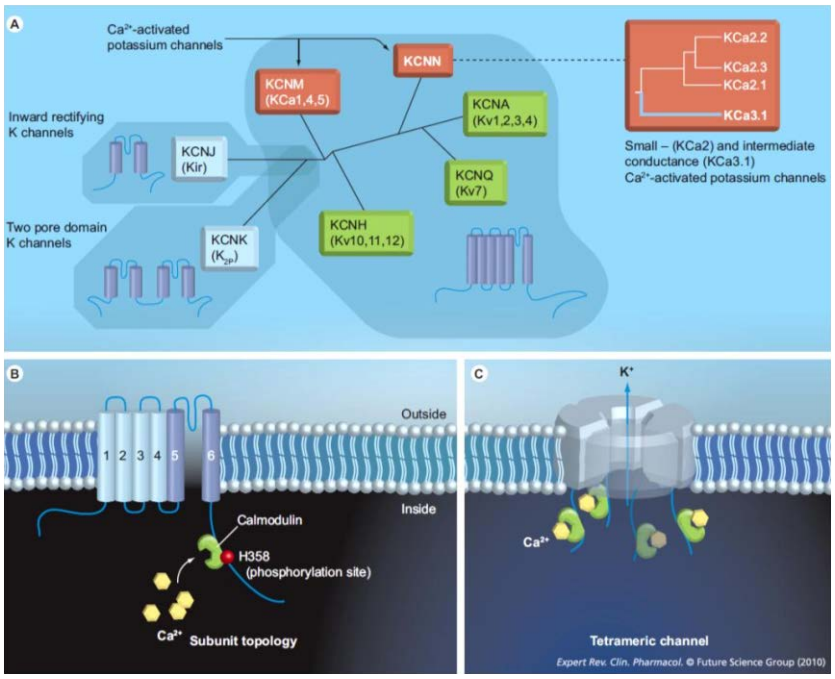

Wulff H et al., Expert Rev Clin Pharmacol (2010)

Figure 1. Properties of KCa3.1 channels. A. Simplified phylogenetic tree of genes for human potassium channel subunits, highlighting in red the two gene families that comprise Ca^{2+}-activated potassium channels and further highlighting the KCNN family which contains the gene for KCa3.1 (KCNN4). B. Illustration of KCa3.1 subunit topology showing the six transmembrane domain signature of this class of channels, along with calmodulin attached to a calmodulin binding domain on the C terminus. The location of the histidine phosphorylation site (H358) known to affect channel activation is also shown. C. Illustration of the homo-tetrameric nature of functional KCa3.1 channels, showing the presence of four calmodulin calcium sensors which accounts for the channel's steep, highly cooperative sensitivity to changes in intracellular calcium concentration.

KCa3.1 gene transcription can be repressed by the repressor element-1 silencing transcription factor[117] and increased through the transcription factors activation protein 1 (AP-1) and Ikaros-2[118]. KCa3.1 function is increased by protein kinase A[119] and nucleoside diphosphate kinase B and inhibited by the histidine phosphatase PHPT1[120]. Nucleoside diphosphate kinase B and PHPT1 directly exert their activity on histidine 358 at the C-terminus and KCa3.1 modulation thus constitutes one of the rare examples of histidine

kinase/phosphatase regulating a biological process in mammals. Clotrimazole and its derivative TRAM-34 are potent and selective inhibitors of KCa3.1. KCa3.1 channels are expressed in a variety of normal and tumor cells, where they participate in important cell functions such as cell cycle progression, migration, and epithelial transport, by controlling the cell volume and the driving force for Ca^{2+} influx[121]. Importantly, TRAM-34 has been already used in several in vivo studies aimed at attenuating restenosis after angioplasty[122], in atherogenesis[123], in EAE[124], in cerebral stroke[125] and other diseases. Another KCa3.1 blocker, ICA17043, has been used in clinical trials for sickle cell anemia and exercise-induced asthma and these trials support KCa3.1 as a safe therapeutic target, with no evident adverse effects even upon long-term use[126].

4.2 Physiological role of KCa3.1

Interesting roles for ion channels in basic biological functions, such as growth control, cell differentiation and migration emerged in studies on normal[127] and malignant cells[104,128]. Glioma cells use ion channels (mainly K^+ and Cl^-), to generate an osmotic gradient for cytoplasmic water flux, thereby altering cellular volume[129]. Important volume changes precede each cell division as glioma cells retract their processes, condense and round up to a sphere[130]. Cell rounding requires the release of cytoplasmic water, accomplished by the coordinated secretion of potassium chloride (KCl) with osmotically obligated water. Outward directed gradients for K^+ and Cl^- are established by the activity of the Na^+/K^+-ATPase and the sodium-potassium-chloride cotransporter isoform-1 (NKCC1), respectively. Intracellular Cl^- reaches concentrations of 100-140 mM, approximately ten-fold higher than that of neurons and other cells[131]. The condensation engages chloride channel-3 (ClC-3)-type channels, which are activated through Ca^{2+}-dependent phosphorylation by Ca^{2+}/CaMKII [132]. K^+ efflux occurs via Ca^{2+}-activated K^+ channels[133] and water leaves through aquaporins[130]. This highly orchestrated interplay of ion transporters and ion channels allows a cell to condense its cell volume rapidly, within approximately 40 minutes, facilitating the pre-mitotic rounding[133]. Similar volume changes occur as gliomas invade the brain through narrow extracellular passageways along white matter tracts or blood vessels. To navigate the tortuous extracellular brain spaces, glioma cells dynamically adjust their volume. On encountering barriers too narrow to pass, cells quickly reduce their volume by approximately 33%, regardless of the size of the barrier. Cell shrinkage is achieved by the

efflux of Cl- ions along with essentially all unbound cytoplasmic water and maximizes the chance of the cell to advance past a barrier. This volume reduction utilizes the same Cl^- and K^+ channels described above[130] and these channels are activated downstream of intracellular Ca^{2+} increases originating from the activation of AMPARs, bradykinin receptors[134] or transient receptor potential channels (TRPC)[135]. The above-described cell volume changes associated with cell migration suggest several new possible pharmacological targets to interfere with glioma invasion. For example, the diuretic bumetanide (Bumax) inhibits intracellular Cl^- accumulation in glioma cells and, in a mouse model, reduced the ability of gliomas to invade and generate satellite tumors[136]. In preclinical studies, the pharmacological inhibition of Cl^- channels or genetic downregulation of ClC-3 reduced the ability of gliomas to invade[137]. Furthermore, the Cl^- channel inhibitor, chlorotoxin, has been used in phase I/II clinical study in patients with glioma[138]. Additionally, the regulators of channels and transporters, such as CaMKII, which regulates ClC-3 KCa^{2+} channels, or the with-no-lysine kinase-3 (WNK3), which regulates[139], may be promising additional targets. It must be emphasized that the hydrodynamic model of glioma invasion assumes that ion channels participate in a facilitator role. Given that cell invasion constitutes a complex and highly coordinated biology, the disruption of only one pathway may not be sufficient to derail the process but could be the first step to build a new combinatorial strategy to counteract glioma cell infiltration in the healthy parenchyma.

4.3 Microglial ion channels

In all living cells, ion channels are required to regulate the membrane potential and intracellular ion concentrations. Functional ion channels allow movements of cations or anions across the membrane, which subsequently may influence a variety of cellular processes, such as proliferation, excitability, migration, apoptosis, secretion and others. Ion channels are specialized membrane proteins that span the plasma membrane. They form hydrophilic pores through which ions flow from one side of the membrane to the other down their electrochemical gradient. Microglial ion channels have been studied using the patch clamp technique. Ion channels can be distinguished based on their ion selectivity, conductances, gating properties, kinetics and pharmacology. Within the CNS, substantial changes in extracellular pH and ion concentrations occur during neuronal activity. For example, the external concentration of potassium increases during neuronal activity and can

be largely augmented under pathological conditions. Changes in the extracellular milieu can dramatically alter the activity of microglial ion channels and subsequently induce changes in microglial functioning and activation.

4.4 Role of KCa3.1 in microglial cells

Many studies on microglial electrophysiology focused on K^+ channels: potassium channels are involved in the regulation of resting potential regulating the majority of their function, such as phagocytosis, antigen presentation, motility, cytokine secretion and others.
Many physiologically active substances increase the concentration of intracellular Ca^{2+}, leading to the activation of Ca^{2+}-activated K^+ channels. These channels are involved in the control of microglia activation and contribute to the upregulation of iNOS and the production of NO and peroxynitrite, directly implicated in neurotoxicity and linked to the activation of mitogen-activated protein kinase (MAPK) cascade[140].
Different brain insults differentially activate microglia; the activation process requires the ability of microglia to change its shape to exert various functions and, as in other cells, also microglia regulate cell shape modulating the concentrations of different ionic species at their inner, trough K+ channels. Also in microglia, KCa3.1 channels are related to different downstream processes, such as migration, activation of specific pathways and neurotoxicity[141,142]. In most cases, the block of KCa3.1 has been shown able to contrast cerebral damage[143] associated with pathologies leading to a reduction of the microglia neurotoxic potential[140]. These important findings raise the awareness that these peculiar channels could be considered as optimal targets for the development of drugs against brain diseases, acting on microglia activation state. Microglia, in fact, is the only cell type expressing KCa3.1 channels in the CNS[141] and the activation of the related current is often considered as a microglia activation parameter[144]. Recently, it has been demonstrated that, upon KCa3.1 inhibition by 1-[(2-Chlorophenyl)diphenylmethyl]-1H-pyrazole (TRAM-34), the glioblastoma multiforme (GBM)- or IL-4-induced profile of microglia/macrophages (M/MΦ) is more polarized toward an inflammatory phenotype. This effect is confirmed, ex vivo, in human specimens from glioma patients and, in vivo, in a mouse model of glioma, where TRAM-34 treatment induced an increase of pro-inflammatory and a reduction of anti-inflammatory gene expression in infiltrating CD11b+ cells. This polarization corresponded

to a reduced tumor size in TRAM-34-treated glioma-bearing mice, further supporting the antitumor effect of inflammatory M/MΦ cells[145].

4.5 KCa3.1 blockers are relatively safe

TRAM-34 (IC50 20 nM) is currently the most widely used pharmacological tool compound for studying the pathophysiology of KCa3.1 because of its high selectivity over other K^+ channels. It was synthesized by Wulff et al.[146] using as a template the antimycotic clotrimazole, which is a potent but poorly tolerated KCa3.1 inhibitor. KCa3.1 blockers are very light immunosuppressants that do not reduce the ability of rodents to eliminate viral infections like influenza[147]. Furthermore, genetic or pharmacological block of KCa3.1 seems relatively safe and well tolerated. KCa3.1 -/- mice were both vital, of normal appearance and normal size of puppies, done do not show any serious anomaly in any of their principal organs, and exhibited rather mild phenotypes: altered volume regulation in erythrocytes and lymphocytes[147], a reduced EDHF (hyperpolarization derived from the endothelium factor), along with a slight increase of ~ 7 mmHg in blood pressure[148] and in thin macrocytosis of erythrocyte and progressive splenomegaly[149]. It has been reported that TRAM-34 has previously been tested for long-term toxicity in mice and rats. In WT C57BL/6L mice, 4 weeks of treatment with 120 mg/kg TRAM-34 i.p. did not induce any changes in body weight, hematology, blood chemistry or necropsy of any major organs. Similarly, treatment of ApoE-/- mice for 3 months did not induce any changes in the body weight, heart weight, blood pressure or heart rate[123]. In male and female Lewis rats, a 6 months toxicity study with 120 mg/kg TRAM-34 did also no induce any changes in body weight, hematology, blood chemistry, necropsy, or increase the susceptibility to infections[150].

Senicapoc, molecule structurally related to TRAM-34, which advanced into Phase-3 clinical trials, has been proven safe and well tolerate in healthy volunteers. It was afterward found to significantly reduce hemolysis and increase hemoglobin levels in a 12-week, multicenter, randomized double-blind Phase-2 study in sickle cell disease patients[151,152].

Brain, Behavior, and Immunity 73 (2018) 584–595

Contents lists available at ScienceDirect

Brain, Behavior, and Immunity

journal homepage: www.elsevier.com/locate/ybrbi

Full-length Article

Ca^{2+}-activated K^+ channels modulate microglia affecting motor neuron survival in $hSOD1^{G93A}$ mice

Germana Cocozza[a,b], Maria Amalia di Castro[a], Laura Carbonari[a], Alfonso Grimaldi[b], Fabrizio Antonangeli[c], Stefano Garofalo[d], Alessandra Porzia[e], Michele Madonna[e], Fabrizio Mainiero[f], Angela Santoni[c,e], Francesca Grassi[a], Heike Wulff[g], Giuseppina D'Alessandro[e,1], Cristina Limatola[d,e,1,*]

[a] Department of Physiology and Pharmacology, Sapienza University, Rome, Italy
[b] Center for Life Nanoscience – Istituto Italiano di Tecnologia@Sapienza, Rome, Italy
[c] Department of Molecular Medicine, Sapienza University, Laboratory affiliated to Istituto Pasteur Italia – Fondazione Cenci Bolognetti, Rome, Italy
[d] Department of Physiology and Pharmacology, Sapienza University, Laboratory affiliated to Istituto Pasteur Italia, Fondazione Cenci Bolognetti, Rome, Italy
[e] IRCCS Neuromed, Pozzilli, IS, Italy
[f] Department of Experimental Medicine, Sapienza University, Rome, Italy
[g] Department of Pharmacology, University of California Davis, Davis, CA 95616, USA

ARTICLE INFO

Keywords:
Microglia
KCa3.1 channels
Motor neurons
Mouse model
ALS
SOD1G93A
Neuromuscolare junction
Spinal cord
Neurodegeneration

ABSTRACT

Recent studies described a critical role for microglia in amyotrophic lateral sclerosis (ALS), where these CNS-resident immune cells participate in the establishment of an inflammatory microenvironment that contributes to motor neuron degeneration. Understanding the mechanisms leading to microglia activation in ALS could help to identify specific molecular pathways which could be targeted to reduce or delay motor neuron degeneration and muscle paralysis in patients. The intermediate-conductance calcium-activated potassium channel KCa3.1 has been reported to modulate the "pro-inflammatory" phenotype of microglia in different pathological conditions. We here investigated the effects of blocking KCa3.1 activity in the $hSOD1^{G93A}$ALS mouse model, which recapitulates many features of the human disease. We report that treatment of $hSOD1^{G93A}$ mice with a selective KCa3.1 inhibitor, 1-[(2-chlorophenyl)diphenylmethyl]-1*H*-pyrazole (TRAM-34), attenuates the "pro-inflammatory" phenotype of microglia in the spinal cord, reduces motor neuron death, delays onset of muscle weakness, and increases survival. Specifically, inhibition of KCa3.1 channels slowed muscle denervation, decreased the expression of the fetal acetylcholine receptor γ subunit and reduced neuromuscular junction damage. Taken together, these results demonstrate a key role for KCa3.1 in driving a pro-inflammatory microglia phenotype in ALS.

1. Introduction

Amyotrophic lateral sclerosis (ALS) is a multifactorial disease characterized by the progressive degeneration of motor neurons (MN) and muscle paralysis. Despite current treatments, patients survive < 3–5 years after the initial diagnosis. Most ALS cases are sporadic (sALS), and only 5–10% have a familial origin (fALS). Among the latter, about 20% express a dominant mutant form of the Cu, Zn superoxide dismutase (SOD1) (Rothstein, 2009). Transgenic mice expressing a mutant SOD1 develop MN pathology, with muscle denervation and weakness similar to ALS patients (Fischer et al., 2004). Many evidence demonstrate that ALS is non-cell autonomous, with multiple co-players involved in disease progression (Robberecht and Philips, 2013). In particular, signals from both glial cells and muscles initiate and sustain MN degeneration (Boillée et al., 2006; Dobrowolny et al., 2008). Neuroinflammation is often associated with ALS (Philips and Robberecht, 2011): microglial reactivity, astrogliosis and lymphocyte infiltration are common in patients and in experimental models of the disease (Hall et al., 1998; Mantovani et al., 2009; Turner et al., 2004). Microglia carrying mutant SOD1 express pro-inflammatory genes, such as *il-1β*, *tnf-α* and *inos* (Philips and Robberecht, 2011; Almer et al., 1999; Henkel et al., 2004). Nevertheless, the exact contribution of neuroinflammation to the pathology of ALS is not clear, possibly acting in concert with additional factors. The knowledge of the molecular mechanisms driving

* Corresponding author at: Sapienza University, Piazzale Aldo Moro 5, 00185 Rome, Italy.
E-mail address: cristina.limatola@uniroma1.it (C. Limatola).
[1] equally contributing authors

https://doi.org/10.1016/j.bbi.2018.07.002
Received 8 May 2018; Received in revised form 28 June 2018; Accepted 2 July 2018
Available online 03 July 2018

the inflammatory responses, and their impact on MN, would be of great importance to develop effective therapeutic treatments. Among the possible modulators of the inflammatory response in the CNS, plasma membrane ion channels are good candidates, regulating membrane potential and intracellular signaling in T cells, B cells and innate immune cells such as macrophages and microglia (Feske et al., 2015; Zierler et al., 2016). In this work, we investigated the role of the intermediate-conductance, Ca^{2+}-activated K^+ channel KCa3.1, in shaping the activation state of microglia in a mouse model of ALS, the $hSOD1^{G93A}$ mice, which recapitulates many features of the human disease. In the CNS, KCa3.1 channels are expressed by microglial cells, where they regulate cell migration and phagocytic activity in physiological and pathological conditions such as glioma, ischemia, spinal cord injury (SCI) and Alzheimer's disease (AD) (Chen et al., 2011; Maezawa et al., 2012; Bouhy et al., 2011; D'Alessandro et al., 2013; Grimaldi et al., 2016). In some conditions (SCI), the expression of KCa3.1 is also reported on astrocytes and neurons (Bouhy et al., 2011). In AD, microglial KCa3.1 potentiate the neurotoxicity induced by oligomeric amyloid-β and lipopolysaccharide (LPS) treatment (Maezawa et al., 2012; Kaushal et al., 2007); while blocking KCa3.1 activity has beneficial effects in rodent models of multiple sclerosis and ischemic stroke, reducing TNF-α and IFN-γ expression in the spinal cord (Reich et al., 2005) or the infarcted area (Chen et al., 2016). The KCa3.1 inhibitor *per se* is not directly neuroprotective in the absence of microglia (Maezawa et al., 2011; D'Alessandro et al., 2016).

In the current study, we treated $hSOD1^{G93A}$ mice with the selective KCa3.1 inhibitor TRAM-34 starting at the pre-symptomatic stage and analyzed the activation state of spinal cord microglia by measuring the expression levels of "pro" and "anti-inflammatory" genes and cell morphology. We found that the chronic inhibition of KCa3.1 activity in $hSOD1^{G93A}$ mice: i) restrained the pro-inflammatory phenotype of microglia; ii) increased the number of healthy MNs; iii) preserved the number of healthy neuromuscular junctions (NMJ) in the *tibialis anterior* muscle; iv) and their maturation level, as assessed by mRNA analysis of AChR γ and ε subunit expression and by current recording on isolated muscle fibres. Furthermore, TRAM-34 treatment delayed motor symptom appearance, as shown by prolonged muscle strength and motor coordination, and increased mice survival. Taken together, these data demonstrate a crucial role for microglia in modulating disease onset and progression, and provide prove-of-concept for the potential targeting of KCa3.1 to reduce ALS-associated neuroinflammation and to protect MNs from degeneration.

2. Materials and methods

2.1. Animal model

The study was conducted in accordance with the ARRIVE guidelines (Kilkenny et al., 2010). All experiments and procedures were approved by the Italian Ministry of Health (authorization n. 78/2017-PR) in accordance with the ethical guidelines on use of animals from the EC Council Directive 2010/63/EU and from the Italian D.Leg 26/2014. All possible efforts were made to minimize animal suffering, and to reduce the number of animals used per condition by calculating the necessary sample size before performing the experiments. hSOD1(G93A) transgenic mice, which express about 20 copies of mutant human $SOD1^{G93A}$ [B6.Cg-Tg(SOD1-G93A)1Gur/J line] were obtained from Jackson Laboratory (Bar Harbor, ME, USA) (RRID:IMSR_JAX:004435) (Charles River, Calco, Italy). B6.Cg-Tg(SOD1-G93A)1Gur/J were also maintained as hemizygotes by breeding transgenic males with wild-type C57BL/6J females from Charles River Laboratories, both maintained on C57BL/6J genetic background. Age-matched non-transgenic C57BL/6J mice were always used as control mice. Only male mice were used for the experiments to minimize gender-induced differences in motor impairment and survival (Choi et al., 2008). Transgenic mice were identified by PCR on DNA obtained from tail biopsies. Briefly, tail tips were digested (overnight, 58 °C) in a buffer containing 100 mM Tris–HCl pH 8, 0.1% SDS 20, 5 mM EDTA pH8, 200 mM NaCl and 20 mg/ml proteinase K (Ambion-Thermo Fisher, Germany, #2548) and the genomic DNA was amplified with SsoFast Eva Green Supermix (Bio-Rad, California, #172-5201) using the following primers: SOD1 forward 5′-CATCAGCCCTAATCCATCTGA-3′; SOD1 reverse 5′- CGCGACTAACA ATCAAAGTGA-3′. Animals were housed in regular polycarbonate cages (30 × 16 × 11 cm), 2–3 per cage, at constant temperature (22 ± 1 °C) and humidity (50%), and were kept on a 12-h light cycle (light 7 a.m.to 7p.m.). Housing comprised nesting objects, with bedding (sawdust) materials. Food (regular chow, containing 14% protein, 5% fat, 3041 kcal ME/kg) and water were freely available. Microbiological analyses were routinely (each 3–4 months) performed and defined endemic Norovirus and Helicobacter in our conventional animal facility. Transgenic animals were weighed two times a week, beginning at 7 weeks of age. Starting at 6 weeks of age mice were evaluated for motor deficits with a behavioral score system: 0 = Full extension of hind legs away from the lateral midline when the mouse is suspended by tail; the mouse must hold this position for 2 s, and is suspended 2–3 times; 1 = Collapse or partial collapse of leg extension towards lateral midline (weakness) or trembling of hind legs during tail suspension; 2 = Curling of the toes and dragging of at least one limb during walking; 3 = Rigid paralysis or minimal joint movement; foot not used for forward motion; 4 = Mouse cannot stand up in 20 s from either side, euthanasia.

Mice were always treated in blinded fashion.

2.2. TRAM-34 treatment and survival analysis

Male transgenic animals were weighed twice a week from 6 until 18 weeks of age. Then, the animal status and weight was monitored daily. Starting at 7 weeks of age, $hSOD1^{G93A}$ mice were randomly grouped (at least 5 mice per experimental group) for vehicle and TRAM-34 (1-[(2-chlorophenyl)diphenylmethyl]-1*H*-pyrazole treatment. Mice were treated daily (early in the morning) with 120 mg/kg of TRAM-34 or the same amount of vehicle (50 µl, peanut oil, Sigma-Aldrich, St. Louis, MO USA, #P2144) by intraperitoneal injections. The treatment regimen was chosen to reach a CNS concentration of TRAM-34 that effectively inhibits KCa3.1 channels, as previously described (D'Alessandro et al., 2013). TRAM-34 was synthesized as described (Wulff et al., 2000). Animals were treated until the age described in the text or until sacrifice for the survival analysis experiments. Animals were sacrificed when unable to stand up within 20 s after being placed on either side.

2.3. Isolation of lumbar microglia cells

Adult microglia were isolated from the lumbar spinal cord tract of age-matched non-transgenic C57BL/6J wt mice (non-tg *wt*) and $hSOD1^{G93A}$ mice as described in (Yip et al., 2009) with minor modifications. Mice were deeply anesthetized with chloral hydrate (i.p., 400 mg/Kg, Carlo Erba Italy, #334085) before being transcardially perfused with phosphate buffered-saline (PBS tablet, Sigma-Aldrich, #P4417). Spinal cords were then flushed out from the spinal canal using a 20 ml syringe filled with PBS and digested with 30 units of papain (15–23 U/mg protein, Sigma-Aldrich, #P3125) for 30 min at 37 °C. Tissue was then triturated with a pipette to obtain single cell suspensions, which were applied to 70-µm/40-µm cell strainers and used for the experiments. Purity of isolated microglia was assessed by morphology and surface staining for $CD11b^+$, $CD45^{low+}$, $Ly6G^-$, $Ly6C^-$. mAbs directly conjugated to PE, PE-Cy7, APC, APC-H7, and PerCP-Cy5.5 fluorochromes and specific for the following antigens (clone name in parentheses) were used: CD45 (1 0 4), CD11b (M1/70), Ly6C (HK1.4), and Ly6G (1A8). Antibodies were from eBioscience (Thermo Fisher, Germany) and BioLegend (San Diego, CA). Immunostaining was performed with saturating amounts of Abs for 30 min

at 4 °C. Purity of isolated microglia cells ranged between 70 and 90 %, as verified by flow cytometry.

2.4. ROS production

Microglia from the lumbar spinal cord of non-tg *wt* mice were treated for 18 h with 5 μM of sodium azide (Acros, part of Thermo Fisher, Germany #190381000) in presence or absence of 2.5 μM of TRAM-34. To evaluate ROS production, cells were extensively washed and incubated with 10 μM of 2′,7′-Dichlorodihydrofluorescein diacetate (DCF, Sigma-Aldrich, #D6883) for 30 min at 37 °C. Cell fluorescence was detected in FL1 channel and analyzed with a FACSCanto II (BD Biosciences). Data were analyzed using FlowJo v9.3.2 software (TreeStar, Ashland, OR, USA).

2.5. Isolation of embryonic mouse MN

MN cultures were obtained from E13 C57BL6/J mice. Pregnant females were euthanized by cervical dislocation and the spinal cords were removed from embryos; tissues were digested with 0.25% Trypsin in Neurobasal medium at 37 °C. After 20 min the reaction was stopped by adding trypsin inhibitor and pipetting 10–15 times with a glass Pasteur pipette, until no more cell aggregates were visible. Cells were kept 15 min at RT on a vibration-free surface and centrifuged at 1200 rpm for 10 min; the pellet was resuspended in complete Neurobasal medium (Gibco, part of Thermo Fisher, Germany #10888-022) (2 mM glutamine, 1% B27, 100 U/ml penicillin and 0.1 mg/mL streptomycin) and plated (2×10^5 cells/well) onto poly-L-lysine coated glass cover slips. After nine days in culture, embryonic mouse MNs (2×10^5 cells/well) were co-cultured with adult microglia (non-tg *wt* pre-treated with 5 μM sodium azide (NaN_3) or $hSOD1^{G93A}$ microglia) plated (10^5 cells/well) on poly-L-lysine-coated transwells (Corning, Sigma-Aldrich, USA, 0.4 μm pore size).

2.6. Microglia/MN co-cultures

Co-cultures were treated with the following: 2.5 μM TRAM-34, or DMSO (0.01%, Sigma-Aldrich, USA) as vehicle. After 72 h of co-culture, MN death was measured by immunofluorescence staining using activated caspase 3 antibody (Cell Signaling, Danvers, USA #9661, 1:400), as apoptotic marker, and non-phosphorylated neurofilament H antibody (SMI32 clone, Biolegend, #801701, 1:500), as MN marker. Only double positive cells were counted as dead cells; this number was normalized to the mean of SMI32-positive cells counted in each well.

2.7. Real-time PCR

Total RNA was extracted from lumbar microglia, muscle fibres of non-tg *wt*, vehicle and TRAM-34-treated $hSOD1^{G93A}$ mice following a standard Trizol (Invitrogen, CA, #T9424) protocol, quantified with NanodropOne (Thermo Scientific) and *retro*-transcripted using IScript Reverse Transcription Supermix (Bio-Rad, #1708841). RT-PCR of genes described was carried out in a I-Cycler IQ Multicolor RT-PCR Detection System (Bio-Rad, #172-5201) using SsoFast Eva Green Supermix (Bio-Rad). Relative gene expression was calculated by ΔΔCT analysis relative to GAPDH expression levels. GAPDH: forward (F), 5′-TCGTCCCGTAG ACAAAATGG-3′, reverse (R), 5′-TTGAGGTCAATGAAGGGGTC- 3′; IL-1β: F, 5′-GCAACTGTTCCTGAACTCAACT-3′, R, 5′-ATCTTTTGGGGTCC GTCAACT-3′; BDNF: F, 5′-CGGC GCCCATGAAAGAAGTA-3′, R, 5′-AGA CCTCTCGAA CCTGCCCT-3′; ARG1:(F), 5′- CTCCAAGCCAAAGTCCTTA GAG-3′, (R) 5′- AGGAGCTGTCATTAGGGACATC-3′; CD163:(F), 5′-TCTGGCTTGACAGCGTTTC-3′, (R) 5′- TGTGTTTGTTGCCTGG ATT-3′;FIZZ:(F),5′-CCAATCCAGCTAACTATCCCTCC-3′, (R) 5′- ACCCA GTAGCAGTCATCCCA-3′;IL-6:(F),5′-GATGGATGCTACCAAACTGGA-3′, (R) 5′-TCTGAAGGACTCTGGCTTTG-3′;INOS:(F), 5′-ACATCGACCCGTC CACAGTAT-3′, (R) 5′- CAGAGGGGTAGGCTTGTCTC-3′;TNF-a:(F), 5′-GTGGAACTGGCAGAAGAG-3′, (R) 5′- CCATAGAACTGATGAG AGG-3′;YM1:(F), 5′-CAGGTCTGGCAATTCTTCTGAA-3′, (R) 5′- GTCTT GCTCATGTGTGTAAGTGA-3′; myogenin (F) 5′-GCACTGGAGTTCGGTC CCA-3′, (R) 5′-GTGATGCTGTCCACGATGGA-3′; atrogyn-1 (F) 5′-GCAG CAGCTGAATAGCATCCA-3′, (R) 5′-GGTGATCGTGAGGCCTTTGAA-3′; AChRγ (F) 5′-GCTCAGCTGCAAGTTGATCTC-3′, (R) 5′-CCTCCTGCTCC ATCTCTGTC-3′; AChRε 5′- GCTGTGTGGATGCTGTGAAC-3′, (R) 5′-GCTGCCCAAAAACAGACATT-3′; kccn4 (F) 5′-GGCTGAAACACCGG AAGCTC-3′, (R) 5′-CAGCTCTGTCAGGGCATCCA-3′.

2.8. Behavioral tests

Mice were housed in standard breeding cages at a constant temperature (22 ± 1∘C) and relative humidity (50%), with a 12:12 h light:dark cycle (light on 07.00–19.00 h). Food and water were available ad libitum. Behavioral tests started when mice were 7 weeks old. All animals were handled for at least 5 min/day for 2–3 days before starting the experiments.

2.8.1. Inverted grid test

Mice were placed in the center of a wire grid (40 × 60 cm, suspended 50 cm above a cushioned table) and then the grid was inverted (maximum time allowed 60 s). The time spent hanging on to the grid was measured. (Rinaldi et al., 2013)

2.8.2. Hindlimb extension reflex

Mice were suspended by the tail, and scored for hindlimb extension reflex deficits. The scores were recorded from 0 to 2 as follows: 2, normal extension reflex in both hind limbs; 1.5, imbalanced extension in the hind limbs; 1.0, extension reflex in only one hindlimb; 0.5, the absence of any hindlimb extension; and 0, total paralysis. (Ludolph et al., 2010)

2.8.3. Hanging wire test

To perform this test, mice were allowed to grab a horizontal wire with their front paws and the time spent hanging measured (maximum time allowed 60 s). Behavior was scored according to the following scale: 1, hanging onto the bar with both forepaws; 2, in addition to 1, attempted to climb onto the bar; 3, hanging onto the bar with two forepaws and one or both hindpaws; 4, hanging onto the bar with all four paws with tail wrapped around the bar; 5, able to walk on the bar to escape. (Rinaldi et al., 2013)

2.8.4. Rotarod test

Motor coordination, strength and balance were assessed using a rotarod apparatus (Ugo Basile, Gemonio Italy, #47650). Animals were placed onto the cylinder at a constant speed of 15 rpm. The arbitrary cut-off time was 300 s., and the longest latency was recorded.

2.8.5. Grip strength test

The apparatus consisted of a grip strength meter (Ugo Basile, #47200), complete with a force transducer and a grasping device (grid for measurement of the four limbs). The mouse was held at the base of the tail and allowed to grab the grid with either four limbs. The mouse was then pulled gently backwards until it released its grip. The peak force of each trial was taken as a measure of the grip strength.

2.9. Immunofluorescence

Spinal cord slices were prepared from $hSOD1^{G93A}$ and non-tg *wt* mice treated with vehicle or TRAM- 34 as described. Spinal cord sections (20 μm) were washed in PBS, blocked (3% goat serum in 0.3% Triton X-100) for 1 h, at RT, and incubated overnight at 4 °C with specific antibodies diluted in PBS containing 1% goat serum and 0.1% Triton X-100. The sections were incubated with the following primary Abs: Iba1 (Wako, Osaka Japan, #019-19741, 1:500), GFAP (Novus

Biologicals, Littleton USA, #NB300-141, 1:500), SMI-32 (BioLegend, 1:500) and cleaved caspase-3 (Cell Signaling, 1:400). After several washes, sections were stained with the fluorophore-conjugated antibody and Hoechst for nuclei visualization and analyzed using a fluorescence microscope. For Iba1/SMI-32 staining, coronal sections were first boiled for 20 min in citrate buffer (pH 6.0) at 95–100 °C.

Quantification of Iba1 and GFAP immunoreactivity was performed on lumbar spinal cord sections (12 serial coronal sections for each animal, in each group, covering the entire L3-L5 segments), using MetaMorph 7.6.5.0 image analysis software (Molecular Device, San Jose USA), after background subtraction. Iba or GFAP immunoreactivity was measured as the ratio of the area occupied by fluorescent cells (thresholded area) versus the total ventral horn area. At least 5 animals per condition were analyzed.

Images were digitized using a CoolSNAP camera (Photometrics, Tucson USA) coupled to an ECLIPSE Ti-S microscope (Nikon, Tokio Japan) and processed using MetaMorph 7.6.5.0 image analysis software (Molecular Device, San Jose USA). Signal co-localization was analyzed measuring the average fluorescence intensity (pixel) of merged signals.

2.10. Motor neuron survival evaluation

For MN survival, the whole ventral horns of lumbar spinal cord were photographed at × 20 magnification and digitized using a CoolSNAP camera (Photometrics) coupled to an ECLIPSE Ti-S microscope (Nikon) and processed using MetaMorph 7.6.5.0 image analysis software (Molecular Device). The number of MNs was evaluated counting only SMI32-positive cells with typical morphology triangular shape, single well-defined axon, large body diameter (≥ 20 μm) and intact axons and dendrites. This was done in 12 serial slices for each animal and data normalized with respect to non-tg wild-type mice, where the number of healthy MNs was taken as 100%.

2.11. Skeleton analysis

Microglia from sections of lumbar ventral horns were analyzed by confocal microscopy using IBA1 signal and skeletonized to assess cell morphology. Twenty μm z-stacks were acquired at 0.5 μm intervals using an FV10i laser scanning microscope (Olympus, Tokyo Japan) at ×60 objective. Cell morphology was measured using a method adapted from Morrison and Filosa, 2013. Maximum intensity projections for the IBA1 channel of each image were generated, binarized, and skeletonized using the Skeletonize 2D/3D plugin in ImageJ, after which the Analyze Skeleton plugin (http://imagej.net/AnalyzeSkeleton) was applied. The average branch number (process end points per cell) for each image with a voxel size exclusion limit of 150 was applied. The number of single and multiple junction points was additionally calculated to give an indication of branching complexity. The areas of the soma and the scanning domain, defined as the perimeter within which individual cells project their dynamic processes, were measured for each cell.

2.12. Fibre preparation

Fibres were obtained from the FDB muscles of hSOD1^{G93A} and non-tg *wt* mice hind-limbs. The dissected muscles were incubated with Type I collagenase (2 mg/ml, Sigma) for 45 min at 37 °C in MEM (Gibco, #11095-080) digestion medium (Sodium Pyruvate 1 mM + FBS 0.2% + Pen Strep 2%, Sigma). After equilibrating in S-MEM (Gibco, #11380-037) Ca2 + -free dissociation medium (Sodium Pyruvate 1 mM + FBS 0.5% + Pen Strep 2% + HEPES 20 mM, Sigma) for 15 min at 37 °C, the muscle fibres were mechanically dissociated using fire polished glass pipettes and P100 micropipette. For recordings, a bunch of single fibres was transferred on ECM (3.33 mg/mL, Sigma-Aldrich, USA) coated glass slide and incubated at 37 °C for 15 min. The fibres remained viable for at least 4–5 h.

2.13. Neuromuscular junction evaluation

Mice treated as above were deeply anaesthetized before being transcardially perfused with PBS. *Tibialis anterior* muscles were dissected out and snap-frozen in cooled isopentane. Muscles were gently stretched on a Sylgard coated Petri dish and fixed with paraformaldehyde 4% in PBS for 60 min at RT. For AChR staining, the fixed muscles were incubated with rhodamine-conjugated alpha-bungarotoxin (6 mg/ml, Molecular Probes, B13423) in FBS-supplemented DMEM 20% for 50 min at 37 °C. Muscle were extensively washed with FBS-supplemented DMEM 20%, then with PBS. Twenty-micrometer serial longitudinal cryosections were collected on poly-lysine coated objective slides (VWR International, Radnor USA) for the quantitative evaluation of NMJ status. Images were digitized using a CoolSNAP camera (Photometrics) coupled to an ECLIPSE Ti-S microscope (Nikon) and processed using MetaMorph 7.6.5.0 image analysis software (Molecular Device). Images of acetylcholine receptors (AChRs) immuno-stained with α-BTX were used for the quantification of NMJ fragmentation. Fragmentation of NMJ was defined as several AChR clusters in small islands with round shape. Average numbers of AChR fragments per NMJ were evaluated. For the quantitative evaluation, about 130 NMJs for each group were analyzed.

2.14. Cell-attached recordings and analysis

Single-channel currents were recorded at room temperature (24–26 °C) in the cell-attached mode from dissociated muscle fibres from hSOD1^{G93A} or non-tg mice and bathed in dissociation medium without divalent ions to prevent contractions. Glass pipettes (3–5 MΩ) pulled with a vertical puller (PC-10, Narishige) were filled with divalent-free NES (NaCl 140 mM, KCl 2.8 mM, Glucose 10 mM, HEPES/NaOH 10 mM, pH 7.3, 295–300 mOsm) plus ACh 200 nM and were connected to a low-noise amplifier (Multiclamp 700B amplifier, Molecular Devices, USA). Data were sampled at 20 kHz and analysed after Gaussian digital filtering at 6 kHz, using a threshold-crossing method (pClamp v. 10.0 software, Axon Instruments), with the detection threshold for channel events set to half-amplitude. Events briefer than 120 μs were incompletely resolved and therefore excluded from the analysis. The histogram of channel amplitudes was adequately fitted by one or two Gaussian distributions and slope conductances were calculated by least-squares linear fitting of unitary current (i)/voltage (V) relationships. Only single openings were used to calculate the mean channel amplitude and the apparent open duration (τop), which was measured at half-amplitude for each event. The kinetic properties of ACh-evoked events were compared at an estimated patch potential of −90 ± 10 mV. Only patch with at least 1000 events were used to perform open channel duration analysis. Results are given as mean ± SEM. The significance of differences was tested by using one-way ANOVA ($P < 0.05$) and Fisher's test.

2.15. Statistical analysis

Data are expressed as the mean ± S.E.M. Student's t-test, paired t-test, Fisher's test, one-way or two-way analysis of variance (ANOVA) was performed. A value of $P < 0.05$ was considered significant. All statistical analyses were carried out using the Sigma Plot 11.0 Software (Systat Software GmbH, Erkrath, Germany). Mouse survival was analyzed with the Kaplan–Meier graph followed by log-rank statistics. The sample size (n) was chosen differently for experiments of animal survival, behavioural tests, electrophysiology, etc, considering the following relation: $n \geq 2\sigma^2 (z_\alpha/D)^2$ where sigma is substituted by an estimate of variance (s2); alpha is at 0.05 (and $Z\alpha = -2$) and D is the difference among treatments.

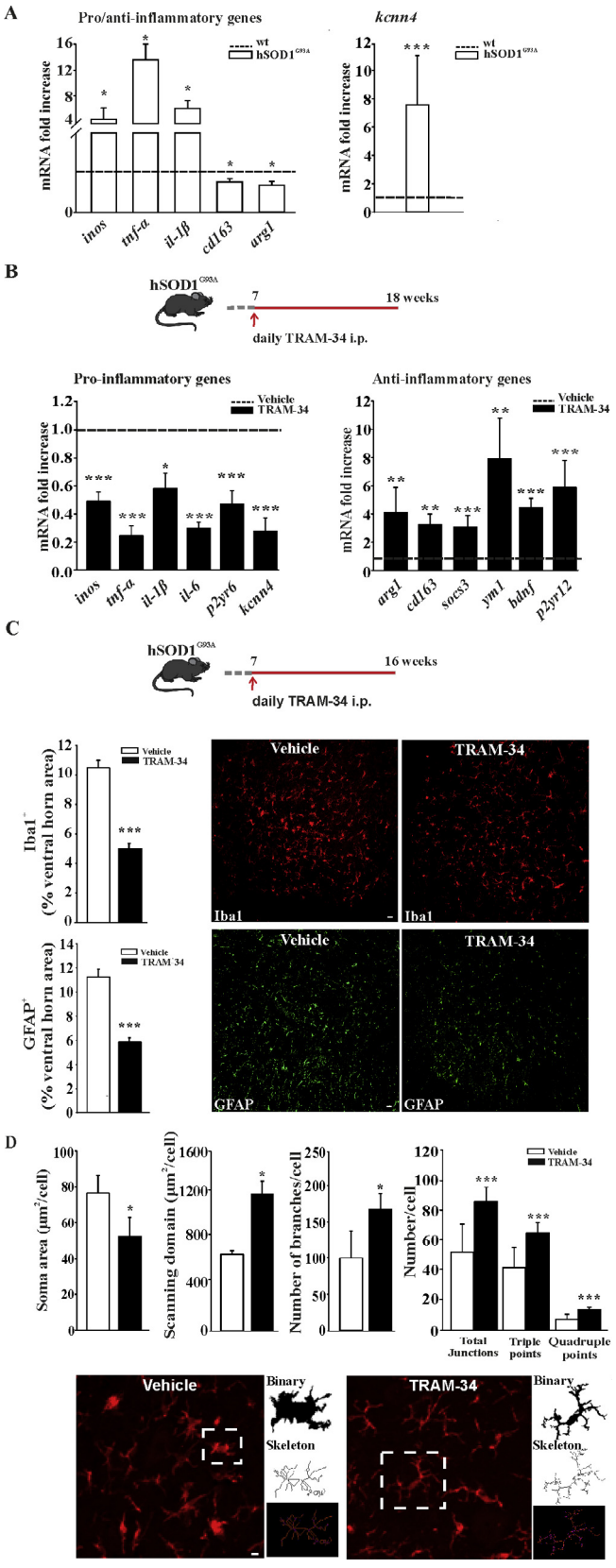

Fig. 1. KCa3.1 channels shape microglia activation in ALS. A: Relative expression level of *inos, tnf-α, il-1β, cd163 and arg1* (left) and *kcnn4* (right) in microglial cells isolated from 18 week-old hSOD1^{G93A} mice compared to each gene in *wt* mice (dotted line) (data are shown as mean ± SEM, n = 3, * < 0.05, *** p < 0.001 *vs wt,* Student's *t* test). B: top, treatment scheme. RT-PCR analyses of the relative expression level of pro- (left) and anti- (right) inflammatory and *kcnn4* genes in microglia cells isolated from the lumbar region of the spinal cord of hSOD1^{G93A} mice expressed as fold increase of TRAM-34-treated *vs* vehicle treated mice (dotted line); data are shown as mean fold increase ± SEM; *p < 0.05, ** p < 0.01, *** p < 0.001 *vs* vehicle by Student's *t*-test n = 6, C: top, treatment scheme. Quantification of Iba1$^+$ (upper panel) and GFAP$^+$ (lower panel) staining in the lumbar region of the spinal cord of vehicle (white bar) and TRAM-34 treated (black bar) mice (data are shown as mean ± SEM. *** p < 0.001 *vs* vehicle by Student's *t* test, n = 5 vehicle, n = 6 TRAM-34). Representative immunofluorescence images are shown on the right (scale bar = 20 μm). D: Morphological analysis of lumbar Iba1$^+$ cells: from left, soma area (TRAM-34 50.92 ± 10.36 μm^2 *vs* vehicle 74.23 ± 9.59 μm^2 *p < 0.002), scanning domain (TRAM-34 1221.75 ± 113.68 μm *vs* vehicle 683.20 ± 35.27 μm *p < 0.010), number of branches per cell (TRAM-34 167.88 ± 21.56 *vs* vehicle 100.50 ± 37.19 ***p < 0.001), junctions (total, 85.56 ± 10.67 *vs* 52.03 ± 18.80; triple, 64.71 ± 7.34 *vs* 41.62 ± 13.66; quadruple 14.02 ± 2.24 *vs* 7.29 ± 3.63 ***p < 0.001) (data are shown as mean ± SEM, 20 cells, 6 slices, 4 mice per condition, by Student's *t*-test). Bottom: representative images of maximum intensity projections of a confocal z-stack imaging of Iba1$^+$ cells, converted to binary images and then skeletonized (scale bar = 20 μm).

3. Results

3.1. KCa3.1 channels modulate spinal microglia in hSOD1^{G93A} mice

In the CNS, KCa3.1 is highly expressed in activated microglia (Kaushal et al., 2007). To investigate the possible involvement of KCa3.1 channels in modulating the phenotype of microglia in the fully symptomatic phase of ALS, we first analyzed the mRNA level of *kcnn4,* by quantitative real time PCR (qRT-PCR), in microglia isolated from the lumbar region of the spinal cord of 18 week-old hSOD1^{G93A} mice. Preliminarily, we confirmed that these cells have increased expression of selected inflammatory genes and reduced expression of anti-inflammatory ones (Fig. 1A, left), as previously described in ALS mice (Liao et al., 2012; Apolloni et al., 2016). We found that hSOD1^{G93A} microglia express high level of *kcnn4* (7.54 fold increase in comparison with age-matched non-tg *wt* mice), suggesting that KCa3.1 channels could play a role in the pro-inflammatory microenvironment observed in ALS (Fig. 1A, right). To directly evaluate the role of KCa3.1 channel activity in modulating microglia phenotype, hSOD1^{G93A} mice were treated with TRAM-34 (daily, 120 mg/kg) from 7 weeks of age (pre-symptomatic stage) until 18 weeks (fully symptomatic stage) (Fig. 1B, top). The long term treatment is not toxic and does not induce changes in body weight, haematology, blood chemistry or necropsy of any major organs, either in mice or rats (Toyama et al., 2008; Chen et al., 2011). After this period, microglial cells were isolated and analyzed as in A. As shown in Fig. 1B, pharmacological KCa3.1 inhibition changed the expression level of several inflammatory genes in hSOD1^{G93A} microglia (left), decreasing *inos, tnf-α, il-1β, il-6* and *p2yr6* expression compared to microglia obtained from vehicle-treated hSOD1^{G93A} mice (dotted line). Interestingly, treatment with TRAM-34 also reduced *kcnn4* expression (to 0.27 ± 0.09 fold) compared to vehicle-treated mice. In contrast, KCa3.1 inhibition increased the expression of the anti-inflammatory genes *arg1, cd163, sosc3, ym1, bdnf* and *p2yr12* (Fig. 1B, right). As a control, we also analyzed gene expression in microglia isolated from the lumbar spinal cord of non-tg *wt* mice, upon vehicle and TRAM-34 (four weeks) treatment. Results obtained indicate that KCa3.1 inhibition induces significant increases of *arg1* and *ym1* genes (see Supplementary Table 2).

Immunofluorescence analysis of the spinal cord, revealed that KCa3.1 inhibition, in hSOD1^{G93A} mice (scheme of mice treatment in

Fig. 1C, top), significantly decreased Iba1 and GFAP staining in the L3-L5 regions, compared to vehicle-treated mice (Fig. 1C, center and bottom), further confirming the induction of a reduced inflammatory environment. Iba1-positive cells in these spinal sections were also analyzed for morphological changes by performing skeleton analysis to quantify single cell shape. The data summarized in Fig. 1D, reveal that Iba-1 positive cells from TRAM-34 treated mice had significantly smaller somas, bigger scanning domains and higher average branch numbers. Skeleton analysis also evidenced higher number of junctions and more triple as well as quadruple junction points, when compared to vehicle-treated animals. Taken together, these results indicate that KCa3.1 inhibition shifts spinal microglia of hSOD1^{G93A} mice towards an anti-inflammatory phenotype and increases the active surveillance that microglia exert in their competence domains. These data consistently support our hypothesis of KCa3.1 involvement in microglia modulation in ALS and further prompted us to verify if channel inhibition could significantly impact disease progression.

3.2. Inhibition of KCa3.1 has beneficial effects in hSOD1^{G93A} mice

To assess the possible beneficial effects of KCa3.1 inhibition on ALS progression, we treated hSOD1^{G93A} mice daily with TRAM-34 or vehicle (as detailed above) from 7-weeks of age until sacrifice (Fig. 2A). Mice were evaluated during the treatment period for changes in weight, locomotor activity, muscle strength, motor coordination and survival. As shown in Fig. 2B, TRAM-34 treatment significantly increased body weight from week 13 to the end stage. Disease onset was retrospectively determined as the age when these mice reached their maximal body weight: KCa3.1 inhibition delayed disease onset of about 3 weeks in hSOD1^{G93A} mice (Fig. 2C). In addition, KCa3.1 inhibition increased survival time (Fig. 2D) compared to vehicle treated mice and significantly prolonged the mean survival time post-paralysis, assessed as the age when mice failed to complete the Rotarod test (Fig. 2E).

We also tested locomotor ability, muscle strength and motor coordination in vehicle and TRAM-34 treated hSOD1^{G93A} mice. The results of these experiments show that in the hanging wire test, the TRAM-34 treated mice (Fig. 2F and G), for the time investigated, always performed with higher scores and spent more time hanging compared to controls. Of note, the TRAM-34-treated mice never reached the lowest score (1) during the symptomatic stage (13–18 weeks), showing a very good, preserved, locomotor ability. In the inverted grid test (Fig. 2H), the average latency to fall recorded for TRAM-34-treated

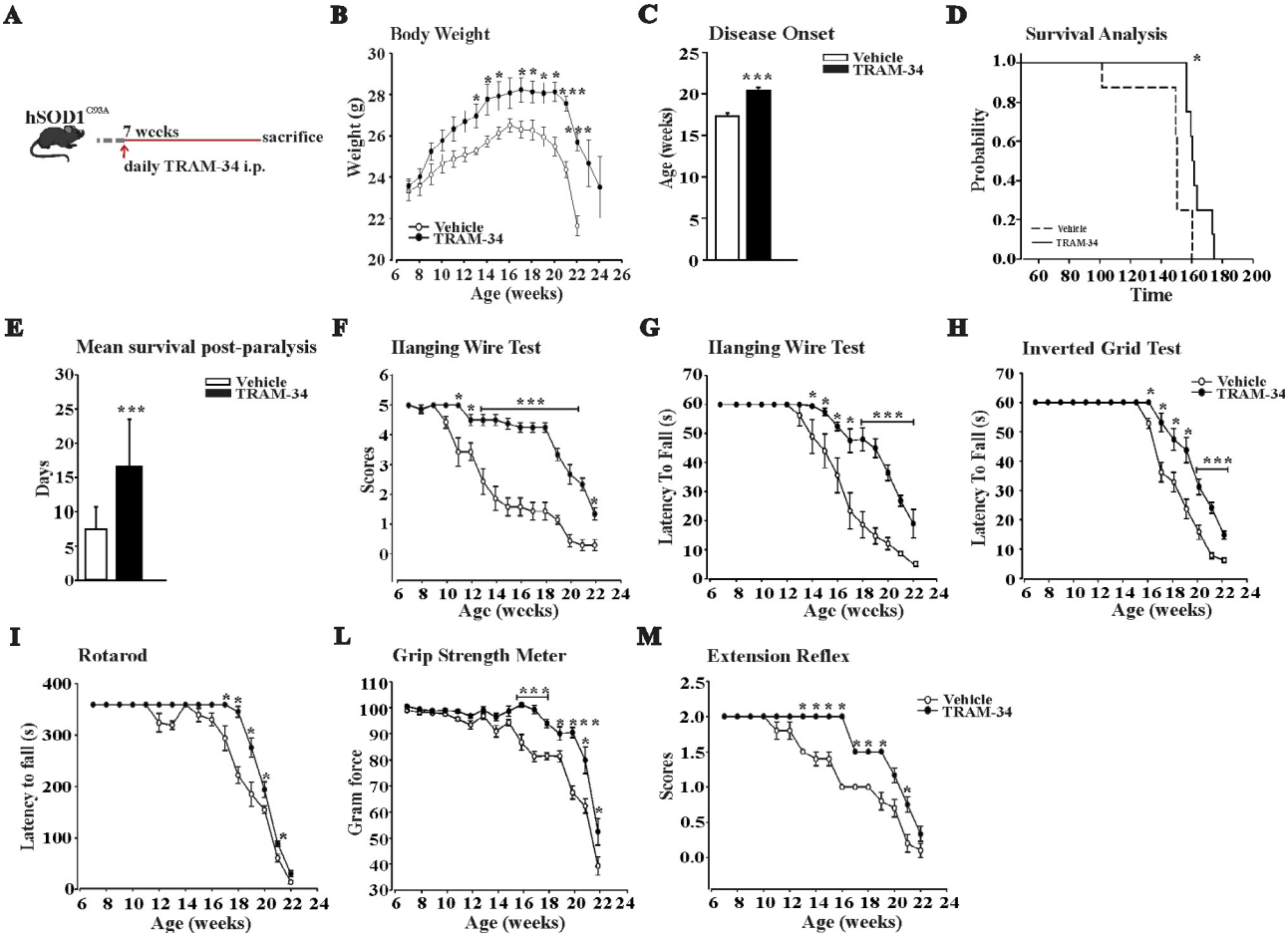

Fig. 2. KCa3.1 channels modulate motor function and survival in hSOD1^{G93A} mice. A: Treatment scheme. B: Variations of body weight over time in vehicle (white) and TRAM-34-treated hSOD1G93A mice (black dots). Data are the mean ± SEM; *p < 0.05, ** p < 0.01, *** p < 0.001 *vs* vehicle by Student's *t*-test n = 9. C: Disease onset index, calculated as the age of peak of body weight. Disease onset in TRAM-34 treated mice was 19.3 ± 0.2 weeks, black bars; in vehicle 16.3 ± 0.2 weeks, white bars. Data are the mean ± SEM *** p < 0.001, n = 9. D: Kaplan–Meier analysis of mice survival. TRAM-34 increased the survival time of hSOD1^{G93A} mice (TRAM-34: 165 ± 2 days; vehicle: 148 ± 7 days, data are the mean ± SEM *p < 0.008 by Log–rank test, n = 9). E: Quantification of the mean survival time post-paralysis. TRAM-34: 16.6 ± 2.41 days (black bar); vehicle: 7.4 ± 0.97 days (white bar) data are the mean ± SEM, n = 9 ***p < 0.001 by Student's *t* test. F-M: Analyses of motor function in SOD1^{G93A} mice treated with TRAM-34 (black dots) or vehicle (white dots) with: hanging wire test, score (F) and latency (G), inverted grid test (H), rotarod test (I), grip strength test (force) (L) and extension reflex (M). Behavioral tests were performed once a week, starting from 7-weeks of age until weeks described in the panels. All behavioral tests were ameliorated by TRAM-34 treatment. Data are expressed as mean ± SEM; *p < 0.05, ** p < 0.01, *** p < 0.001 *vs* vehicle hSOD1^{G93A} mice by Student's *t*-test n = 9.

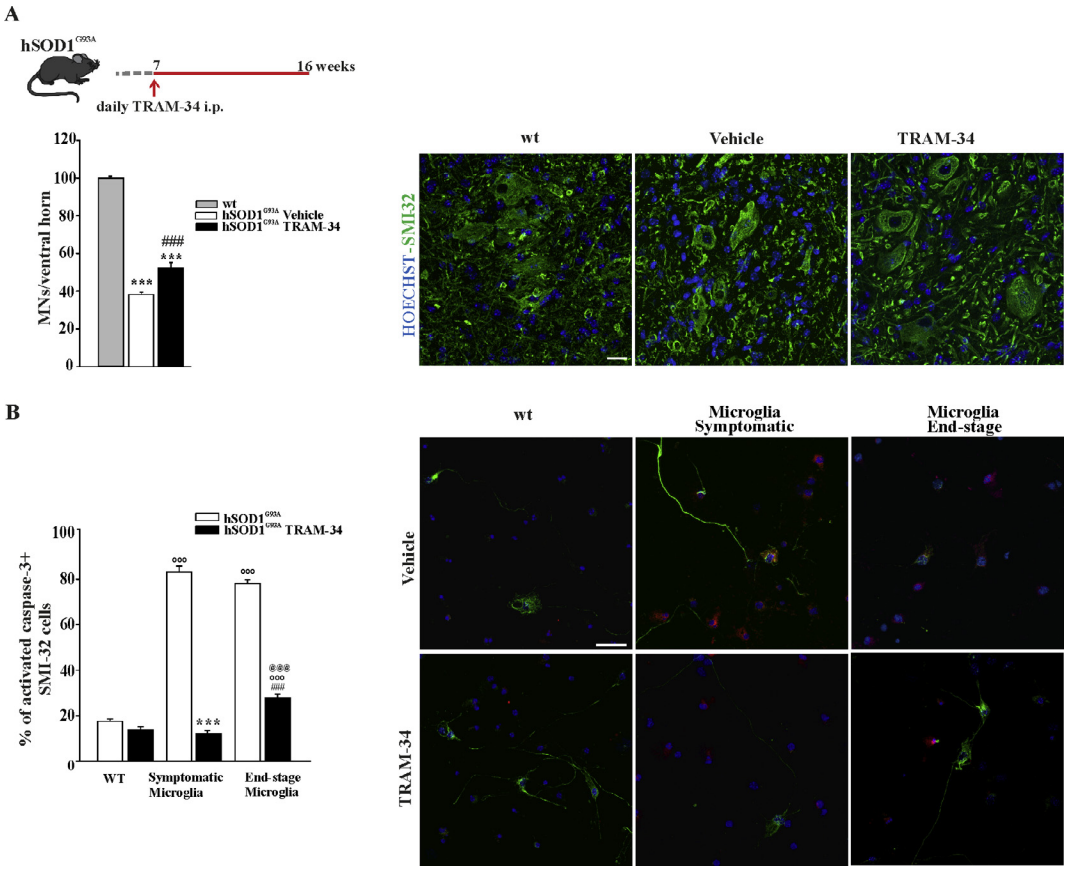

Fig. 3. KCa3.1 channels modulate microglia-motor neuron interaction in hSOD1^{G93A} mice. A: top, treatment scheme. Bottom, quantification of MNs (counted as SMI-32 stained cells in the ventral horns of the spinal cord) in non-tg *wt*, and hSOD1^{G93A} mice treated with vehicle or TRAM-34. Data are shown as mean ± SEM ***p < 0.001 *vs wt;* ###p < 0.001 *vs* vehicle by One Way ANOVA, TRAM-34n = 6; Vehicle n = 5; *wt* n = 3). Representative immunofluorescence images are shown on the right (scale bar = 20 μm). B Non-tg *wt* MNs co-cultured with microglia isolated from the spinal cord of *wt*, symptomatic or end-stage hSOD1^{G93A} mice treated with TRAM-34 (2.5 μM, black bars) or DMSO (white bars). After 72 h, MN death was quantified counting the activated caspase 3/SMI32 double positive cells. Data are mean ± SEM; n = 3 in triplicate, °°°p < 0.001 *vs wt* microglia, ***p < 0.001 *vs* symptomatic microglia, ###p < 0.001 *vs* end-stage microglia, @@@ p < 0.001 *vs wt* microglia + TRAM-34 by Two Way ANOVA (Holm-Sidak method): Representative immunofluorescence images are shown on the right (scale bar = 20 μm).

mice was longer compared to vehicle-treated mice at all the time point analyzed. hSOD1^{G93A} mice were further tested for motor coordination and balance using a Rotarod apparatus. Mice treated with TRAM-34 performed better on the Rotarod (Fig. 2I) and continued to do so until week-21. The grip strength data (Fig. 2L) obtained for TRAM-34 treated mice showed that the rate of muscle deterioration was lower compared to vehicle treated mice, suggesting a slower disease progression. In addition, mice treated with TRAM-34 showed a preserved hind-limb extension reflex (Fig. 2M) compared to vehicle treated mice from the beginning of the symptomatic stage. Taken together, these results show that KCa3.1 inhibition significantly delays symptom onset, suggesting that these channels are involved in accelerating disease progression.

3.3. Motor neurons are protected by selective KCa3.1 inhibition in hSOD1^{G93A}mice

In order to investigate if the activity of KCa3.1 channels in microglia could be involved in MN death in ALS, another group of hSOD1^{G93A} mice were treated with TRAM-34 or vehicle from the pre-symptomatic until the disease onset phase (from 7 weeks to 16 weeks of age, scheme on top of Fig. 3A) when the spinal cords were collected. MNs in the ventral horns of the spinal cord regions L3-L5 were stained with an antibody against the non-phosphorylated neurofilament H (SMI32) (a MN marker) and cells with large cell body (diameter ≥ 20 μm) were counted. The mean number of MNs in *wt* animals was taken as control value. As shown in Fig. 3A, KCa3.1 inhibition, in hSOD1^{G93A} mice, increased MN survival (TRAM-34 52.00 ± 3.13%, vehicle 38.26 ± 1.38% *vs wt* 100 ± 1.09%). Taking advantage of a microglia/MN co-culture system, we then evaluated the specific communication between MN and microglial cells. To this aim, primary adult microglia isolated from symptomatic (16 weeks) or end-stage (> 20 weeks) hSOD1^{G93A} mice were co-cultured with MNs isolated from the spinal cord of mouse embryos (E13) and treated with 2.5 μM TRAM-34 or vehicle (DMSO). After 72 h of co-culture, MN death was measured by staining with SMI32 and the activated caspase 3 antibody, as an apoptosis marker. As shown in Fig. 3B, co-cultures with both symptomatic and end-stage hSOD1^{G93A} microglia induced MN death (apoptotic MNs in symptomatic and end-stage were respectively, 83.3 ± 2.5% and 78.1 ± 1.6%), while co-culture with *wt* microglia did not (apoptotic MNs were 17.8 ± 1.7%), in accordance with (Frakes et al., 2014). In the presence of the KCa3.1 inhibitor, MN death induced by hSOD1^{G93A} microglia was prevented or significantly decreased (symptomatic microglia: 12.1 ± 1.4%; end-stage: 28 ± 1.5%; *wt*: 17.8 ± 1.7%). These data indicate that KCa3.1 channel activity on microglia influences microglia-MN communication, increasing MN death in hSOD1^{G93A} mice.

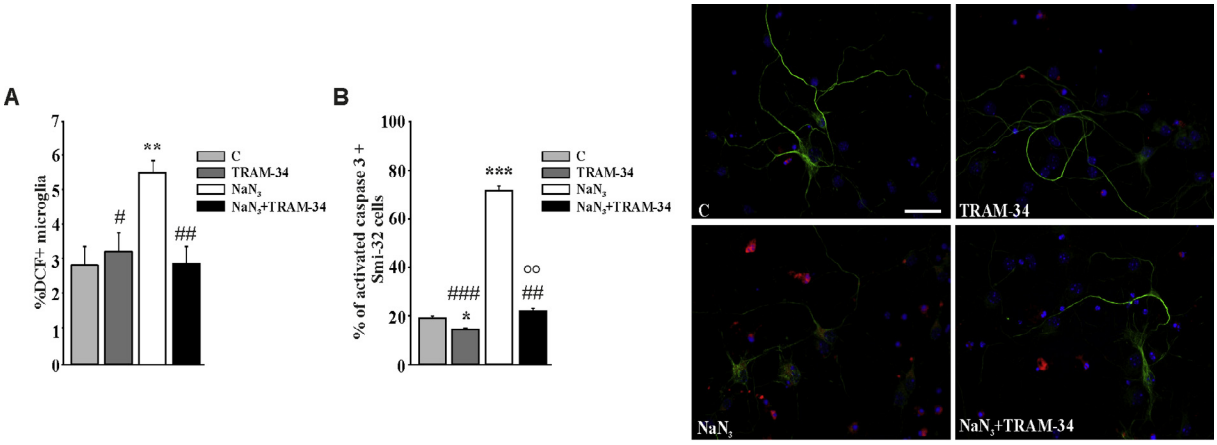

Fig. 4. MNs are protected against ROS neurotoxicity by TRAM-34 treated microglia. A: Quantification of ROS production in non-tg *wt* microglia treated with NaN_3 (5 μM), vehicle (DMSO, control) or TRAM-34 (2.5 μM) for 18 h, measured as dichlorofluorescein positive cells by cytofluorimetry (Data are expressed as % of DCF^+ microglia, mean ± SEM, n = 3 in triplicate, **p = 0.005 *vs* C; #p = 0.048, ##p = 0.004 *vs* NaN_3 by Two Way ANOVA (Holm-Sidak method). B: Cell death quantification of MNs co-cultured for 24 h with non-tg wt microglia pre-treated as in A. Data are expressed as % of active-caspase 3/SMI32 double positive cells on SMI32 positive cells in each condition and are the mean ± SEM. n = 3 in triplicate, ***p < 0.001, *p = 0.037 *vs* control, ## p = 0.003, ### p < 0.001 *vs* NaN_3, °°p = 0.003 *vs* TRAM-34 by Two Way ANOVA (Holm-Sidak method). Representative immunofluorescence images are shown on the right (scale bar = 20 μm).

3.4. Selective KCa3.1 inhibition counteracts ROS-induced microglia neurotoxicity

Mitochondrial reactive oxygen species (ROS) play a prominent role in the oxidative stress observed in ALS (Barber et al., 2010). To investigate whether KCa3.1 activity modulates ROS production in microglia, we used sodium azide (NaN_3), an inhibitor of the electron transport chain, to increase ROS levels (Ye et al., 2016). Microglia (from *wt* mice) were therefore treated with 5 μM NaN_3 for 18 h, in the presence or absence of TRAM-34 (2.5 μM) or vehicle, and mitochondrial ROS production was evaluated by loading cells with 10 μM 2′,7′-dichlorofluorescin diacetate (DCF). Alternatively, microglia were co-incubated for additional 24 h with primary MN to evaluate neurotoxicity.

The data reported in Fig. 4A show that NaN_3 treatment induced ROS production in microglia and that KCa3.1 channel inhibition reduced it, as measured by cytofluorimetric analysis (DCF^+ microglial cells were: NaN_3: 5.4 ± 0.3%; NaN_3 + TRAM-34: 2.8 ± 0.4%). In accordance, MN death (measured as above) increased when MNs were co-cultured for 48 h with microglia pre-treated with NaN_3 (Fig. 4B, 19.06 ± 0.8% control microglia; 71.6 ± 2.04% NaN_3 microglia). Neurotoxicity was abolished when MNs were co-cultured with microglia pre-treated with NaN_3/TRAM-34 (22.06 ± 1.98%), suggesting that KCa3.1 function is involved in sustaining ROS production in microglia. As shown in the first two bars of Fig. 4B, TRAM-34 exerted a minor neuroprotective action also in control co-cultures.

3.5. Selective KCa3.1 inhibition preserves neuromuscular junction (NMJ) functionality

In $hSOD1^{G93A}$ mice, muscle force and motor coordination start to decline at about 10–11 weeks, with clear evidence of NMJ alterations (Dobrowolny et al., 2011). The functional data reported above suggest that NMJ is preserved for longer time in animals treated with TRAM-34. Therefore, we performed morphological and functional analysis of NMJ in $hSOD1^{G93A}$ mice treated with TRAM-34 or vehicle from 7-to 16-weeks of age (Fig. 5A, left). To evaluate the NMJ morphology/integrity, the *tibialis anterior* (TA) muscle was isolated, stretched and fixed. Bundles of muscle fibres were stained with alpha-bungarotoxin (α-BTX) and analyzed for NMJ fragmentation. In symptomatic, vehicle treated mice, the average acetylcholine receptor (AChR)-rich fragments per NMJ were 2.07 ± 0.18 (vehicle n = 3, 136 NMJs) and in TRAM-34-treated $hSOD1^{G93A}$ mice this value drops to 0.96 ± 0.06 (TRAM-34n = 4, 135 NMJs), not dissimilar to what was observed in non-tg age matched mice (0.4 ± 0.06 per NMJ, non-tg n = 3, 148 NMJs) (see Fig. 5A, center and right for representative images).

Several signaling pathways contribute to skeletal muscle atrophy in ALS patients as well as in $hSOD1^{G93A}$ mice (Krasnianski et al., 2005; Dupuis et al., 2006). Increased expression of the late myogenic transcription factor myogenin *(myf4)* and the muscle-specific E3 ubiquitin ligase (*atrogin 1*) were detected in both mouse (Manzano et al., 2011) and human ALS muscles (Léger et al., 2006). As shown in Fig. 5B, the mRNA level of *atrogin1* and *myogenin* were reduced in TRAM-34- *vs* vehicle-treated $hSOD1^{G93A}$ mice (respectively 0.27-fold and 0.69-fold; vehicle n = 3 TRAM-34n = 4 *atro gin* *p < 0.002 *vs* vehicle, *myogenin* ***p < 0.001 *vs* vehicle).

We also measured the expression level of AchRγ and ε subunits in vehicle and TRAM-34 treated mice, an index for NMJ denervation (Martinou and Merlie, 1991). In $hSOD1^{G93A}$ muscle, at the paralysis stage, expression of AChRγ was upregulated, in agreement with previous studies (Krasnianski et al., 2005). Data reported in Fig. 5C show a decreased (0.59-fold) AChR γ and an increased (3.08-fold) AChR ε expression in TRAM-34 treated $hSOD1^{G93A}$ mice (vehicle n = 4 TRAM-34n = 6, AChRγ ***p < 0.001 *vs* vehicle, AChRε ***p < 0.001 *vs* vehicle).

To assess whether TRAM-34 treatment preserves AChR functionality, patch-clamp recordings were performed in acutely dissociated flexor *digitorum brevis* (FDB) muscle fibres. The single channel properties of AChRs were investigated under cell-attached conditions at the end-plate region. To improve the mechanical stability of the patches, recordings were performed with pipette solutions free of Ca^{2+} and Mg^{2+} ions. In all recordings obtained from *wt* mice (13 fibres/5 animals) only one population of ACh-activated channels was observed (Fig. 5D, left). Unitary channel slope conductance was 78.23 ± 1.71 pS, as expected for AChRε in the absence of divalent cations. By contrast, in 7 out of 11 recordings obtained in end-plates from 16-weeks old, vehicle treated $SOD1^{G93A}$ mice (5 mice) two population of channels, differing in amplitude, were observed (Fig. 5D, middle). Slope conductances were 53.15 ± 1.96 pS (23%) and 82.56 ± 1.28 pS (77%), typical values for γ- and ε- containing AChRs, respectively. As expected, based on the data reported above, only one population of ACh-evoked channel openings was detected in 10 out of 12 recordings (6 mice) in TRAM-34 treated $hSOD1^{G93A}$ mice (Fig. 5D, right). Channel slope conductance was 79.22 ± 1.75 pS. In 2 fibres, a

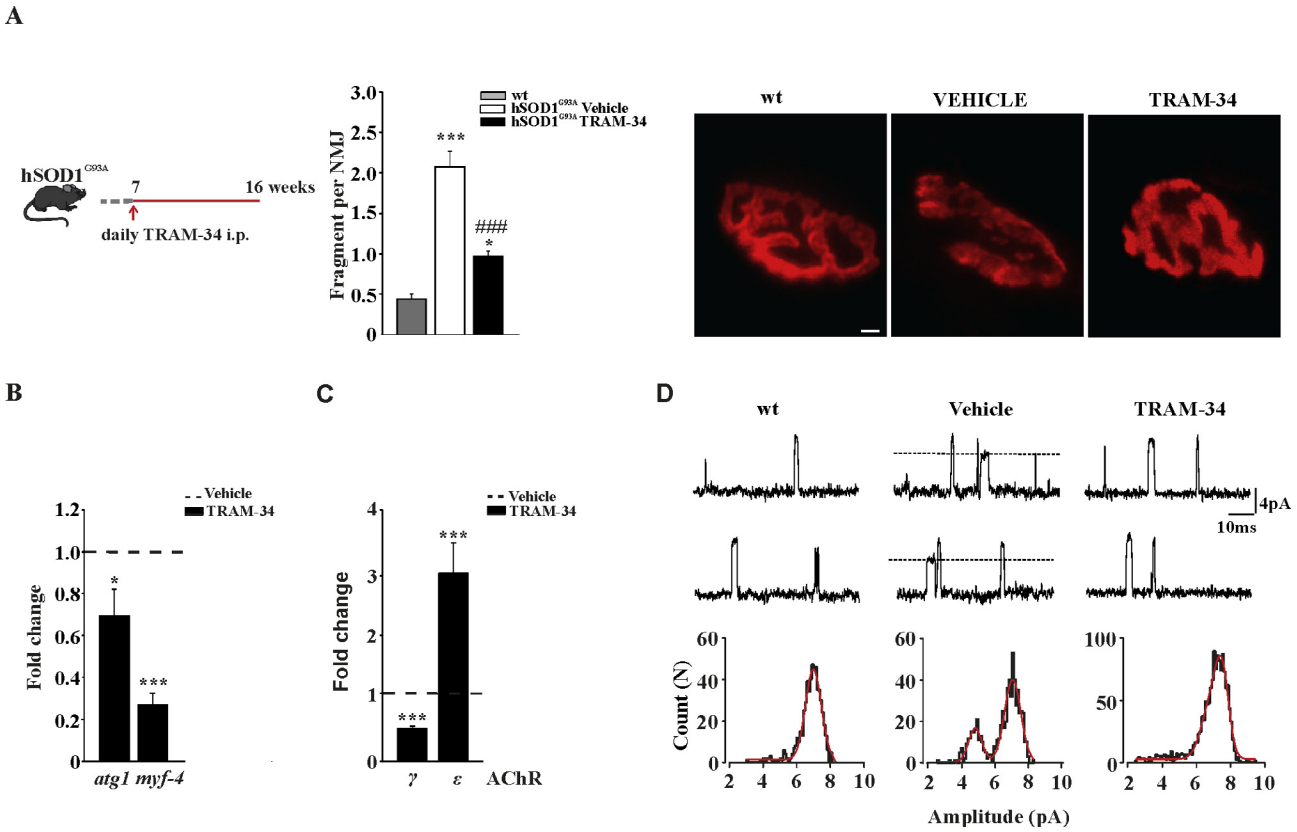

Fig. 5. KCa3.1 channel inhibition ameliorates NMJs functionality. A: left, treatment scheme. Center, AChR fragments per NMJ in the different conditions, as indicated (mean ± SEM, n = 4 mice; *p < 0.05, ***p < 0.001 *vs wt*, ###p < 0.001 *vs* vehicle; 130 α-BTX-positive NMJ per group were randomly chosen and analyzed). Right, representative images of *tibialis anterior* (TA) muscles stained with α-BTX for each experimental group (scale bar = 20 μm). B: Relative expression of *atg1* and *myf4* in the TA muscle of 16-weeks old mice. Data are normalized to GAPDH and expressed as fold changes ± SEM *vs* vehicle treated hSOD1^{G93A} mice (n = 3–4). C: Relative expression of γ and ε AChR in TA muscles from vehicle and TRAM-34-treated hSOD1^{G93A} mice. Data are normalized to GAPDH and expressed as fold changes ± SEM *vs* vehicle. D: Single channel recordings of (ACh)-evoked unitary events in *FDB* muscle fibres dissociated from non-tg, vehicle and TRAM-34 treated hSOD1^{G93A} mice. In the top and middle, non-consecutive traces recorded in an end-plate evoked by ACh (200 μM) at an estimated patch potential of −85 mV. Dotted lines indicate openings of ACh-γ found only in vehicle hSOD1^{G93A} mice. Lower, histograms of the of unitary events, best fitted by two Gaussian functions (continuous line) only in the vehicle hSOD1^{G93A} group.

small fraction of openings belonged to a population with 38.1 and 59.34 pS slope conductance. Thus, the number of fibres expressing AChRγ channel was significantly reduced in TRAM-34-treated hSOD1^{G93A} mice ($p = 0.0009$, Fisher's exact test). The slope conductance of AChRε showed no statistically significant difference among groups. The histograms of AChRε channel open duration were fitted to the sum of three exponential components which did not differ among the groups (Suppl. Table 1) showing that the function of AChR channels is not perturbed in hSOD1^{G93A} mice.

4. Discussion

Increasing evidence supports the hypothesis that in ALS, a neuroinflammatory microenvironment support MN degeneration (Fiala et al., 2010; Puentes et al., 2016; Pasetto et al., 2017; Vallarola et al., 2018). In this paper we demonstrated that in hSOD1^{G93A}, a mouse model of fALS, spinal microglia overexpress the calcium-activated potassium channel, KCa3.1, and that blockade of this channel induces a significant delay in the appearance of all symptoms, preserving motor function and slowing disease progression. In the CNS, KCa3.1 is expressed by microglia and transformed cells (Kaushal et al., 2007; Manzano et al., 2011) and, in a model of spinal cord injury, it has been detected on neurons and astrocytes (Bouhy et al., 2011). In our experimental conditions, we never measured KCa3.1 activity or expression in spinal MN of *wt* and hSOD1^{G93A} mice. KCa3.1 channels expressed on microglial cell play important roles in neurodegenerative diseases and in brain tumors modulating cell phenotype (D'Alessandro et al., 2018; Nguyen et al., 2017). The expression of the mutant SOD1^{G93A} gene in microglia has been related to MN degeneration and to ALS progression (Boillée et al., 2006; Beers et al., 2006). Here we tested the hypothesis that the activity of KCa3.1 channels is associated to a pro-inflammatory phenotype of microglial cells, that favors MN death and disease progression. This is the first study that investigate the role of KCa3.1 channels in ALS, and we demonstrated that the chronic treatment of hSOD1^{G93A} mice with the KCa3.1 channel inhibitor TRAM-34 modulates the phenotype of spinal microglia. In both ALS patients and mouse models, the expression of pro-inflammatory genes increases (Lu et al., 2016; Lee et al., 2016), while anti-inflammatory genes decrease (Liao et al., 2012; Apolloni et al., 2016; Lewis et al., 2014). In line with our hypothesis, we observed that TRAM-34 treatment reverts this trend, increasing the anti-inflammatory (such as *arg1, cd163, socs3*, and *ym1*) and decreasing several pro-inflammatory genes (*il1β, tnf-α, il6* and *inos*) in spinal microglia of hSOD1^{G93A} mice. Interestingly, KCa3.1 blockade induces some phenotypic changes also in microglia of *wt* mice, increasing the expression of *arg1* and *ym1* genes, further confirming the role of this channel in the modulation of microglia phenotype. Like in other neurodegenerative diseases and similarly to brain tumors, microglia play a dual role in early and late stages of ALS (Ferreira and Bernardino, 2015). A recent data-driven experimental approach revealed a link between microglia and the development of MN pathology, identifying soluble TREM2 in the CSF as a putative marker of disease progression (Cooper-Knock et al., 2017).

Expression of other genes, potentially relevant to microglia function and MN death, is also altered by blockade of KCa3.1 channels, in agreement with the induction of an anti-inflammatory phenotype. For example, the expression of the *p2yr6* gene is increased in spinal hSOD1^{G93A} microglia (D'Ambrosi et al., 2009), and we observed that TRAM-34 treatment prevents this overexpression. P2Y6 purinergic receptors are involved in microglia phagocytosis (Koizumi et al., 2007; Brown and Neher, 2014) and related to MN loss in ALS (D'Ambrosi et al., 2009). The phagocytic activity of microglia has debated roles in ALS, where it controls the removal of MNs at different stages of the disease (D'Ambrosi et al., 2009; Butovsky et al., 2014). Interestingly, recent data (Paolicelli et al., 2017), demonstrate that TDP-43, a gene associated with ALS, controls microglia phagocytic activity.

The expression of BDNF, insulin-like growth factor-1 (IGF-1), fibroblast growth factor-2 (FGF-2), and vascular endothelial growth factor are all downregulated in ALS patients (Shruthi et al., 2017; Ohsawa et al., 2010). We observed that the expression of the neuroprotective factor *bdnf* is boosted in hSOD1^{G93A} microglia by inhibiting KCa3.1 activity.

In line with the gene expression data, spinal microglia of TRAM-34 treated hSOD1^{G93A} mice at symptomatic stage are less amoeboid, have smaller soma and higher branching complexity. These morphology data reveal that blockade of KCa3.1 activity restores the patrolling activity of microglia in hSOD1^{G93A} mice. This is in accordance with the higher expression of the metabotropic receptor P2Y12, known to be involved in microglia process mobility (Appel et al., 2011).

Microglia-MN communication in hSOD1^{G93A} mice also benefits from the blockade of KCa3.1 channels. The observed neuroprotective effect is likely due to the combination of a reduced inflammatory phenotype and an increased production of the neurotrophin BDNF. Taken together, these data confirm a key role for KCa3.1 in mediating a pro-inflammatory microglia behavior, as described in other CNS diseases, such as AD, multiple sclerosis, spinal cord injury and ischemia (Maezawa et al., 2011; Moloney et al., 2014; Kaushal et al., 2007; Chen et al., 2016).

These findings are associated with a reduced NMJ damage, seen as less fragmented and better-preserved structure, together with a decreased muscle denervation, demonstrated by a shift in the expression of the γ and ε AChR subunits in hSOD1^{G93A} mice treated with TRAM-34. We interpret the enhanced expression of the ε AChR subunit as a consequence of ongoing denervation/reinnervation cycles in TRAM-34 treated mice. Functional recordings on FDB fibres confirmed the expression data. In addition, KCa3.1 inhibition induced a decrease in the expression markers of atrophy normally detected in ALS muscle (Dobrowolny et al., 2011), such as myogenin and the E3 ubiquitin ligase atrogin 1.

Degeneration of NMJs together with multiple pathogenic mechanisms such as oxidative stress, aberrant protein aggregation, defective axonal transport, neuroinflammation and mitochondrial dysfunction, all contribute to MN failure in ALS (Philips and Robberecht, 2011; Barber and Shaw, 2010; Blokhuis et al., 2013; Barber et al., 2006). In particular, mitochondrial ROS play a prominent role in the oxidative stress observed in ALS (Barber and Shaw, 2010). We used low concentrations of sodium azide to block the electron transport chain and to induce effects on microglia neurotoxic properties (see Ye et al., 2016), and observed that KCa3.1 inhibition prevented the consequent increase in ROS production in microglial cells. Notably, in addition to the plasma membrane, KCa3.1 (and other Ca^{2+} activated potassium channels such as KCa1.1) are also expressed in the inner membrane of the mitochondria in transformed cells and cardiomyocytes (De Marchi et al., 2009; Aldakkak et al., 2010). KCa1.1 activation increases respiration and ROS generation in cardiac cells providing protection against ischemia and reperfusion (IR) injury (Stowe et al., 2006). We hypothesize that, at least the effect of KCa3.1 inhibition on ROS production, could be partially due to the perturbation of K^+ homeostasis between the mitochondrial matrix and the inter membrane space.

It has been shown that, in GBM, histamine activates KCa3.1 channels through cell hyperpolarization, which in turn induces Ca^{2+} influx (Fioretti et al., 2009); clemastine, a histamine receptor (H1R) antagonist, ameliorates ALS pathology modulating inflammatory parameters (Apolloni et al., 2016). Our results are in accordance with a possible mechanism where histamine, released by peripheral mast cells, activates KCa3.1; blocking H1R would also reduce KCa3.1 activity, thus affecting ALS progression.

4.1. Conclusions

In conclusion, our data indicate that the blockade of KCa3.1, when initiated in the pre- symptomatic stage of the disease, elicits broad protective effects in hSOD1^{G93A} mice inducing: i) anti-inflammatory phenotype in microglia, that re-acquire a proper scanning domain; ii) reduced MN degeneration; iii) an overall delay of disease onset and motor dysfunction and iv) increased mean survival time. Overall, these data describe, for the first time, a critical role for KCa3.1 activity in modulating ALS onset and progression, at least in the hSOD1^{G93A} murine model investigated here. It remains to be clarified: i) whether the effect of the blockade of KCa3.1 on hSOD1^{G93A} mice could be relevant in other familiar forms of ALS, and in sALS; ii) the involvement of other target cells such as immune cells or other parenchymal cells. As a potential future application, it is worth to mention that a molecule structurally related to TRAM-34, Senicapoc®, which advanced into Phase-3 clinical trials, has been proven safe in humans (Ataga et al., 2011). Our data demonstrate that KCa3.1 is a potential target to counteract neuroinflammation and neuromuscular degeneration, at least in familial ALS.

Acknowledgments

The authors thank Maria Teresa Ciotti for embryonal motor neuron cultures. This work was supported by Italian Ministry of University and Research [PRIN 2015] to C.L.; by the National Institute of Health [R01 NS098328 (NINDS)] to H.W. C.L is fellow of the Synanet Network (Twinning Project H2020).

Competing interests

No competing interests declared.

Appendix A. Supplementary data

Supplementary data associated with this article can be found, in the online version, at https://doi.org/10.1016/j.bbi.2018.07.002.

References

Aldakkak, M., Stowe, D.F., Cheng, Q., Kwok, W.M., Camara, A.K., 2010. Mitochondrial matrix K^+ flux independent of large-conductance Ca^{2+}-activated K^+ channel opening. Am. J. Physiol. Cell Physiol. 298, C530–C541.

Almer, G., Vukosavic, S., Romero, N., Przedborski, S., 1999. Inducible nitric oxide synthase up-regulation in a transgenic mouse model of familial amyotrophic lateral sclerosis. J. Neurochem. 72 (6), 2415–2425.

Apolloni, S., Fabrizio, P., Parisi, C., Amadio, S., Volonte, C., 2016. Clemastine confers neuroprotection and induces an anti-inflammatory phenotype in SOD1(G93A) mouse model of amyotrophic lateral sclerosis. Mol. Neurobiol. 53, 518–531.

Appel, S.H., Zhao, W., Beers, D.R., Henkel, J.S., 2011. The microglial-motoneuron dialogue in ALS. Acta Myol. 30 (1), 4–8.

Ataga, K.I., Reid, M., Ballas, S.K., Yasin, Z., Bigelow, C., James, L.S., Smith, W.R., Galacteros, F., Kutlar, A., Hull, J.H., Stocker, J.W., Study Investigators, 2011. Improvements in haemolysis and indicators of erythrocyte survival do not correlate with acute vaso-occlusive crises in patients with sickle cell disease: a phase III randomized, placebo-controlled, double-blind study of the Gardos channel blocker senicapoc (ICA-17043). Br. J. Haematol. 153, 92–104.

Barber, S.C., Shaw, P.J., 2010. Oxidative stress in ALS: key role in motor neuron injury and therapeutic target. Free Radic. Biol. Med. 48 (5), 629–641.

Barber, S.C., Mead, R.J., Shaw, P.J., 2006. Oxidative stress in ALS: a mechanism of neurodegeneration and a therapeutic target. BBA 1762 (11–12), 1051–1067.

Beers, D.R., Henkel, J.S., Xiao, Q., Zhao, W., Wang, J., Yen, A.A., Siklos, L., McKercher,

S.R., Appel, S.H., 2006. Wild-type microglia extend survival in PU. 1 knockout mice with familial amyotrophic lateral sclerosis. Proc. Natl. Acad. Sci. U.S.A. 103, 16021–16026.
Blokhuis, A.M., Groen, E.J., Koppers, M., van den Berg, L.H., Pasterkamp, R.J., 2013. Protein aggregation in amyotrophic lateral sclerosis. Acta Neuropathol. 125, 777–794.
Boillée, S., Yamanaka, K., Lobsiger, C.S., Copeland, N.G., Jenkins, N.A., Kassiotis, G., Cleveland, D.W., 2006. Onset and progression in inherited ALS determined by motor neurons and microglia. Science 312, 1389–1392.
Bouhy, D., Ghasemlou, N., Lively, S., Redensek, A., Rathore, K.I., Schlichter, L.C., Samuel, D., 2011. Inhibition of the Ca^{2+}-dependent K^+ channel, KCNN4/KCa3.1, improves tissue protection and locomotor recovery after spinal cord injury. J. Neurosci. 31, 16298–16308.
Brown, G.C., Neher, J.J., 2014. Microgli al phagocytosis of live neurons. Nat. Rev. Neurosci. 15, 209–216.
Butovsky, O., Jedrychowski, M.P., Cialic, R., Krasemann, S., Murugaiyan, G., Fanek, Z., Greco, D.J., Wu, P.M., Doykan, C.E., Kiner, O., Lawson, R.J., Frosch, M.P., Pochet, N., Fatimy, R.E., Krichevsky, A.M., Gygi, S.P., Lassmann, H., Berry, J., Cudkowicz, M.E., Weiner, H.L., 2014. Targeting miR-155 restores abnormal microglia and attenuates disease in SOD1 mice. Ann. Neurol. 77, 75–99. https://doi.org/10.1002/ana.24304.
Chen, Y.J., Raman, G., Bodendiek, S., O'Donnell, M.E., Wulff, H., 2011. The KCa3.1 blocker TRAM-34 reduces infarction and neurological deficit in a rat model of ischemia/reperfusion stroke. J. Cereb. Blood Flow Metab. 31, 2363–2374.
Chen, Y.J., Nguyen, H.M., Maezawa, I., Grössinger, E.M., Garing, A.L., Köhler, R., Jin, L.W., Wulff, H., 2016. The potassium channel KCa3.1 constitutes a pharmacological target for neuroinflammation associated with ischemia/reperfusion stroke. J. Cereb. Blood Flow Metab. 36 (12), 2146–2161.
Choi, C.I., Lee, Y.D., Gwag, B.J., Cho, S.L., Kim, S.S., Suh-Kim, H., 2008. Effects of estrogen on lifespan and motor functions in female hSOD1 G93A transgenic mice. J. Neurol. Sci. 268 (1–2), 40–47.
Cooper-Knock, J., Gren, C., Altschuler, G., Wei, W., Bury, J.J., Heath, P.R., Wyles, M., Gelsthorpe, C., Highley, J.R., Lorente-Pons, A., Beck, T., Doyle, K., Otero, K., Traynor, B., Kirby, J., Shaw, P.J., Hide, W.A., 2017. A data-driven approach links microglia to pathology and prognosis in amyotrophic lateral sclerosis. Acta Neuropathol. Commun. 5 (1), 23.
D'Alessandro, G., Catalano, M., Sciaccaluga, M., Chece, G., Cipriani, R., Rosito, M., Grimaldi, A., Lauro, C., Cantore, G., Santoro, A., Fioretti, B., Franciolini, F., Wulff, H., Limatola, C., 2013. KCa3.1 channels are involved in the infiltrative behavior of glioblastoma in vivo. Cell Death Dis. 4, e773.
D'Alessandro, G., Limatola, C., Catalano, M., 2018. Functional roles of the Ca^{2+}-activated K^+ channel, KCa3.1, in brain tumors. Curr Neuropharmacol 2017 Jul 13.
D'Ambrosi, N., Finocchi, P., Apolloni, S., Cozzolino, M., Ferri, A., Padovano, V., Pietrini, G., Carrì, M.T., Volonté, C., 2009. The proinflammatory action of microglial P2 receptors is enhanced in SOD1 models for amyotrophic lateral sclerosis. J. Immunol. 183, 4648–4656.
De Marchi, U., Sassi, N., Fioretti, B., Catacuzzeno, L., Cereghetti, G.M., Szabò, I., Zoratti, M., 2009. Intermediate conductance Ca^{2+}-activated potassium channel (KCa3.1) in the inner mitochondrial membrane of human colon cancer cells. Cell Calcium 45 (5), 509–516.
Dobrowolny, G., Aucello, M., Rizzuto, E., Beccafico, S., Mammucari, C., Boncompagni, S., Belia, S., Wannenes, F., Nicoletti, C., Del Prete, Z., Rosenthal, N., Molinaro, M., Protasi, F., Fano, G., Sandri, M., Musaro, A., 2008. Skeletal muscle is a primary target of SOD1G93A-mediated toxicity. Cell Metab. 8, 425–436.
Dobrowolny, G., Aucello, M., Musarò, A., 2011. Muscle atrophy induced by SOD1G93A expression does not involve the activation of caspase in the absence of denervation. Skelet Muscle 1 (1), 3.
Dupuis, L., Gonzalez De Aguilar, J.L., Echaniz-Laguna, A., Loeffler, J.P., 2006. Mitochondrial dysfunction in amyotrophic lateral sclerosis also affects skeletal muscle. Muscle Nerve 34, 253–254.
Ferreira, R., Bernardino, L., 2015. Dual role of microglia in health and disease: pushing the balance toward repair. Front. Cell. Neurosci. 9, 51.
Feske, S., Wulff, H., Skolnik, E.Y., 2015. Ion channels in innate and adaptive immunity. Annu. Rev. Immunol. 33, 291–353.
Fiala, M., Chattopadhay, M., La Cava, A., Tse, E., Liu, G., Lourenco, E., Eskin, A., Liu, P.T., Magpantay, L., Tse, S., Mahanian, M., Weitzman, R., Tong, J., Nguyen, C., Cho, T., Koo, P., Sayre, J., Martinez-Maza, O., Rosenthal, M.J., Wiedau-Pazos, M., 2010. IL-17 is increased in the serum and in spinal cord CD8 and mast cells af ALS patient. J Neuroinflammation 7, 76.
Fioretti, B., Catacuzzeno, L., Sforna, L., Aiello, F., Pagani, F., Ragozzino, D., Castigli, E., Franciolini, F., 2009. Histamine hyperpolarizes human glioblastoma cells by activating the intermediate-conductance Ca^{2+}-activated K^+ channel. Am. J. Physiol. Cell Physiol. 297 (1), C102–C110.
Fischer, L.R., Culver, D.G., Tennant, P., Davis, A.A., Wang, M., Castellano-Sanchez, A., Khan, J., Polak, M.A., Glass, J.D., 2004. Amyotrophic lateral sclerosis is a distal axonopathy: evidence in mice and man. Exp. Neurol.. 185, 232–240.
Frakes, A.E., Ferraiuolo, L., Haidet-Phillips, A.M., Schmelzer, L., Braun, L., Miranda, C.J., Ladner, K.J., Bevan, A.K., Foust, K.D., Godbout, J.P., Popovich, P.G., Guttridge, D.C., Kaspar, B.K., 2014. Microglia induce motor neuron death via the classical NF-kappaB pathway in amyotrophic lateral sclerosis. Neuron 81 (5), 1009–1023.
Grimaldi, A., D'Alessandro, G., Golia, M.T., Grössinger, E.M., Di Angelantonio, S., Ragozzino, D., Santoro, A., Esposito, V., Wulff, H., Catalano, M., Limatola, C., 2016. KCa3.1 inhibition switches the phenotype of glioma-infiltrating microglia/macrophages. Cell Death Dis. 7, e2174.
Hall, E.D., Oostveen, J.A., Gurney, M.E., 1998. Relationship of microglial and astrocytic activation to disease onset and progression in a transgenic model of familial ALS. Glia 23, 249–256.
Henkel, J.S., Engelhardt, J.I., Siklós, L., Simpson, E.P., Kim, S.H., Pan, T., Goodman, J.C., Siddique, T., Beers, D.R., Appel, S.H., 2004. Presence of dendritic cells, MCP-1, and activated microglia/macrophages in amyotrophic lateral sclerosis spinal cord tissue. Ann. Neurol. 55, 221–235.
Kaushal, V., Koeberle, P.D., Wang, Y., Schlichter, L.C., 2007. The Ca^{2+}-activated K^+ channel KCNN4/KCa3.1 contributes to microglia activation and nitric oxide-dependent neurodegeneration. J. Neurosci. 27, 234–244.
Kilkenny, C., Browne, W.J., Cuthill, I.C., Emerson, M., Altman, D.G., 2010. Improving bioscience research reporting: the ARRIVE guidelines for reporting animal research. PLoS Biol. 8 (6), e1000412.
Koizumi, S., Shigemoto-Mogami, Y., Nasu-Tada, K., Shinozaki, Y., Ohsawa, K., Tsuda, M., Joshi, B.V., Jacobson, K.A., Kohsaka, S., Inoue, K., 2007. UDP acting at P2Y6 receptors is a mediator of microglial phagocytosis. Nature 446, 1091–1095.
Krasnianski, A., Deschauer, M., Neudecker, S., Gellerich, F.N., Müller, T., Schoser, B.G., Krasnianski, M., Zierz, S., 2005. Mitochondrial changes in skeletal muscle in amyotrophic lateral sclerosis and other neurogenic atrophies. Brain 128, 1870–1876.
Lee, J., Park, J., Kim, S., Park, I., Seo, Y.S., 2016. Differential regulation of neuronal and inducible nitric oxide synthase (NOS) in the spinal cord of mutant SOD1 (G93A) ALS mice. Biochem. Biophys. Res. Commun. 387 (1), 202–206.
Léger, B., Vergani, L., Sorarù, G., Hespel, P., Derave, W., Gobelet, C., D'Ascenzio, C., Angelini, C., Russell, A.P., 2006. Human skeletal muscle atrophy in amyotrophic lateral sclerosis reveals a reduction in Akt and an increase in atrogin-1. FASEB J. 20, 583–585.
Lewis, K.E., Rasmussen, A.L., Bennett, W., King, A., West, A.K., Chung, R.S., Chuah, M.I., 2014. Microglia and motor neurons during disease progression in the SOD1G93A mouse model of amyotrophic lateral sclerosis: changes in arginase1 and inducible nitric oxide synthase. J. Neuroinflammation 11, 55.
Liao, B., Zhao, W., Beers, D.R., Henkel, J.S., Appel, S.H., 2012. Transformation from a neuroprotective to a neurotoxic microglial phenotype in a mouse model of ALS. Exp. Neurol. 237, 147–152.
Lu, C.H., Allen, K., Oei, F., Leoni, E., Kuhle, J., Tree, T., Fratta, P., Sharma, N., Sidle, K., Howard, R., Orrell, R., Fish, M., Greensmith, L., Pearce, N., Gallo, V., Malaspina, A., 2016. Systemic inflammatory response and neuromuscular involvement in amyotrophic lateral sclerosis. Neurol. Neuroimmunol. Neuroinfl. 3 (4), e244.
Ludolph, A.C., Bendotti, C., Blaugrund, E., Hengerer, B., Löffler, J.P., Martin, J., Meininger, V., Meyer, T., Moussaoui, S., Robberecht, W., Scott, S., Silani, V., Van Den Berg, L.H., 2010. ENMC Group for the Establishment of Guidelines for the Conduct of Preclinical and Proof of Concept Studies in ALS/MND Models. Guidelines for preclinical animal research in ALS/MND: a consensus meeting. Amyotroph. Lateral Scler. 11, 38–45.
Maezawa, I., Zimin, P.I., Wulff, H., Jin, L.W., 2011. Amyloid-beta protein oligomer at low nanomolar concentrations activates microglia and induces microglial neurotoxicity. J. Biol. Chem. 2011 (286), 3693–3706.
Maezawa, I., Jenkins, D.P., Jin, B.E., Wulff, H., 2012. Microglial KCa3.1 channels as a potential therapeutic target for Alzheimer's disease. Int. J. Alzheimer Dis 868972.
Mantovani, S., Garbelli, S., Pasini, A., Alimonti, D., Perotti, C., Melazzini, M., Bendotti, C., Mora, G., 2009. Immune system alterations in sporadic amyotrophic lateral sclerosis patients suggest an ongoing neuroinflammatory process. J. Neuroimmunol. 210, 73–79.
Manzano, R., Toivonen, J.M., Oliván, S., Calvo, A.C., Moreno-Igoa, M., Muñoz, M.J., Zaragoza, P., García-Redondo, A., Osta, R., 2011. Altered expression of myogenic regulatory factors in the mouse model of amyotrophic lateral sclerosis. Neurodegener. Dis. 8, 386–396.
Martinou, J.C., Merlie, J.P., 1991. Nerve-dependent of acetylcholine receptor epsilon-subunit gene expression. J. Neurosci. 11, 1291–1299.
Moloney, E.B., de Winter, F., Verhaagen, J., 2014. ALS as a distal axonopathy: molecular mechanisms affecting neuromuscular junction stability in the presymptomatic stages of the disease. Front. Neurosci. 8, 252.
Morrison, H.W., Filosa, J.A., 2013. A quantitative spatiotemporal analysis of microglia morphology during ischemic stroke and reperfusion. J. Neuroinflammation 10, 1–20.
Nguyen, H.M., Grössinger, E.M., Horiuchi, M., Davis, K.W., Jin, L.W., Maezawa, I., Wulff, H., 2017. Differential Kv1.3, KCa3.1, and Kir2.1 expression in "classically" and "alternatively" activated microglia. Glia 65, 106–121.
Ohsawa, K., Irino, Y., Sanagi, T., Nakamura, Y., Suzuki, E., Inoue, K., Kohsaka, S., 2010. P2Y12 receptor-mediated integrinβ1 activation regulates microglial process extension induced by ATP. Glia 58, 790–801.
Paolicelli, R.C., Jawaid, A., Henstridge, C.M., Valeri, A., Merlini, M., Robinson, J.L., Rose, J., Appel, S., Lee, V.M., Trojanowski, J.Q., Spires-Jones, T., Schulz, P.E., Rajendran, L., 2017. TDP-43 depletion in microglia promotes amyloid clearance but also induces synapse loss. Neuron 95 (2), 297–308.e6.
Pasetto, L., Pozzi, S., Castelnovo, M., Basso, M., Estevez, A.G., Fumagalli, S., De Simoni, M.G., Castellaneta, V., Bigini, P., Restelli, E., Chiesa, R., Trojsi, F., Monsurrò, M.R., Callea, L., Maleševic, M., Fischer, G., Freschi, M., Tortarolo, M., Bendotti, C., Bonetto, V., 2017. Targeting extracellular Cyclophilin A Reduces neuroinflammation and extends survival in a mouse model of amyotrophic lateral sclerosis. J. Neurosci. 37 (6), 1413–1427.
Philips, T., Robberecht, W., 2011. Neuroinflammation in amyotrophic lateral sclerosis: role of glial activation in motor neuron disease. Lancet Neurol. 10, 253–263.
Puentes, F., Malaspina, A., van Noort, J.M., Amor, S., 2016. Non-neuronal cells in ALS: role of glial, immune cells and blood-CNS barriers. Brain Pathol. 26, 248–257.
Reich, E., Cui, L., Yang, L., Pugliese-Sivo, C., Golovko, A., Petro, M., Vassileva, G., Chu, I., Nomeir, A.A., Zhang, L.K., Liang, X., Kozlowski, J.A., Narula, S.K., Zavodny, P.J., Chou, C.C., 2005. Blocking ion channel KCNN4 alleviates the symptoms of experimental autoimmune encephalomyelitis in mice. Eur. J. Immunol. 35, 1027–1036.
Rinaldi, A., Defterali, C., Mialot, A., Garden, D.L., Beraneck, M., Nolan, M.F., 2013. HCN1 channels in cerebellar Purkinje cells promote late stages of learning and constrain

synaptic inhibition. J. Physiol. 591, 5691–5709.
Robberecht, W., Philips, T., 2013. The changing scene of amyotrophic lateral sclerosis. Nat. Rev. Neurosci. 14, 248–264.
Rothstein, J.D., 2009. Current hypotheses for the underlying biology of amyotrophic lateral sclerosis. Ann. Neurol. 65 (Suppl. 1), S3–S9.
Shruthi, S., Sumitha, R., Varghese, A.M., Ashok, S., ChandrasekharSagar, B.K., Sathyaprabha, T.N., Nalini, A., Kramer, B.W., Raju, T.R., Vijayalakshmi, K., Alladi, P.A., 2017. Brain-Derived neurotrophic factor facilitates functional recovery from ALS-cerebral spinal fluid-induced neurodegenerative changes in the NSC-34 motor neuron cell line. Neurodegener. Dis. 17 (1), 44–58.
Stowe, D.F., Aldakkak, M., Camara, A.K., Riess, M.L., Heinen, A., Varadarajan, S.G., Jiang, M.T., 2006. Cardiac mitochondrial preconditioning by big Ca^{2+}- sensitive K^+ channel opening requires superoxide radical generation. Am. J. Physiol. Heart Circ. Physiol. 290, H434–H440.
Toyama, K., Wulff, H., Chandy, K.G., Azam, P., Raman, G., Saito, T., Fujiwara, Y., Mattson, D.L., Das, S., Melvin, J.E., Pratt, P.F., Hatoum, O.A., Gutterman, D.D., Harder, D.R., Miura, H., 2008. The intermediate-conductance calcium-activated potassium channel KCa3.1 contributes to atherogenesis in mice and humans. J. Clin. Invest. 118, 3025–3037.
Turner, M.R., Cagnin, A., Turkheimer, F.E., Miller, C.C., Shaw, C.E., Brooks, D.J., Leigh, P.N., Banati, R.B., 2004. Evidence of widespread cerebral microglial activation in amyotrophic lateral sclerosis: an [11C](R)-PK11195 positron emission tomography study. Neurobiol. Dis. 15 (3), 601–609.
Vallarola, A., Sironi, F., Tortarolo, M., Gatto, N., De Gioia, R., Pasetto, L., De Paola, M., Mariani, A., Ghosh, S., Watson, R., Kalmes, A., Bonetto, V., Bendotti, C., 2018. RNS60 exerts therapeutic effects in the SOD1 ALS mouse model through protective glia and peripheral nerve rescue. J Neuroinflammation 15 (1), 65.
Wulff, H., Mark, J., Miller, Wolfram Hänsel, Grissmer, Stephan, Cahalan, Michael D., George Chandy, K., 2000. Design of a potent and selective inhibitor of the intermediate-conductance Ca^{2+}-activated K^+ channel, IKCa1: a potential immunosuppressant. Proc. Natl. Acad. Sci. 97, 8151–8156.
Ye, J., Jiang, Z., Chen, X., Liu, M., Li, J., Liu, N., 2016. Electron transport chain inhibitors induce microglia activation through enhancing mitochondrial reactive oxygen species production. Exp. Cell Res. 340 (2), 315–326.
Yip, P.K., Kaan, T.K., Fenesan, D., Malcangio, M., 2009. Rapid isolation and culture of primary microglia from adult mouse spinal cord. J. Neurosci. Methods 183 (2), 223–237.
Zierler, S., Sumoza-Toledo, A., Suzuki, S., Dúill, F.Ó., Ryazanova, L.V., Penner, R., Ryazanov, A.G., Fleig, A., 2016. TRPM7 kinase activity regulates murine mast cell degranulation. J. Physiol. 594 (11), 2957–2970.

CONCLUSIONS AND PERSPECTIVES

In this paper we report for the first time that spinal microglia overexpress the calcium-activated potassium channel, KCa3.1, in hSOD1^{G93A} mice, a model of familial ALS; it is well known that this channel is involved in several physiological and pathological cellular functions[121]. We found that the chronic inhibition of KCa3.1 activity in hSOD1^{G93A} mice: i) attenuates the pro-inflammatory phenotype of microglia; ii) increases the number of healthy MNs; iii) preserves the number of healthy neuromuscular junctions (NMJ) in the tibialis anterior muscle; iv) and their maturation level, as assessed by mRNA analysis of AChR γ and ε subunit expression and by current recording on isolated muscle fibers. Furthermore, TRAM-34 treatment delays motor symptoms appearance, as shown by prolonged muscle strength and motor coordination, and increases mice survival. In this work, we focused on the effect of KCa3.1 blockade in one mouse model of ALS. However, SOD1 transgenic mice are extensively used as preclinical models to test therapeutic strategies. The pathological alterations found in SOD1 mice are correlated with features in patient tissues and important information on ALS pathology derived from studies on this model. Unfortunately, many of the therapeutic strategies, based on single study observations in rodent mutant SOD1 models, failed in a mostly sporadic ALS population[153]. To our advantage it is important to stress that, the blockade of KCa3.1, in several pathological conditions[141,143], has been shown able to counteract cerebral damage associated with pathologies leading to a reduction of the microglia neurotoxic potential. In AD, microglial KCa3.1 potentiates the neurotoxicity induced by oligomeric amyloid-β and lipopolysaccharide (LPS) treatment[140,141], while blocking KCa3.1 activity has beneficial effects in rodent models of multiple sclerosis and ischemic stroke, reducing TNF-α and IFN-γ expression in the spinal cord[150] or the infarcted area[125]. The KCa3.1 inhibitor per se is not directly neuroprotective in the absence of microglia, indicating a good microglia specificity, and has no toxic effects in rodents[123,125]. These important findings raise the awareness that these peculiar channels could be considered as optimal targets for the development of drugs against brain diseases, acting on microglia activation state. To corroborate and generalize our pre-clinical findings, we plan to use others familial models of ALS to evaluate the role of KCa3.1 in the inflammatory response. Among the possible modulators of the inflammatory response in the CNS, plasma membrane ion channels are good candidates, regulating membrane potential and intracellular signaling also in T cells, B cells and innate immune cells such as macrophages [154,155]. It would be interesting to investigate the

involvement of KCa3.1 activity in inflammatory response also in these cells in the context of ALS. Another important aspect that we plan to re-consider in the future work is the disease time-window in which to study the effect of KCa3.1 activity on inflammatory response. We plan to inhibit channel activity not only before the onset of symptoms, but also later considering that the majority ALS patients in clinical trials always surpassed the onset of disease. In this case, positive results will be more relevant for the clinical setting, even though treatment during the presymptomatic phase already gave us important information concerning the preventive effects of KCa3.1 inhibition in a mouse model of ALS. KCa3.1 inhibition induces a moderate extension on lifespan, likely due to the multi-systemic nature of ALS disease in which neuronal and metabolic impairments have been detected and multiple cell types are involved. Nevertheless, the robust effect of KCa3.1 inhibition on neuroinflammation warrants further investigation on its value as add-on therapy in ALS. In fact, a TRAM-34 analogue (Senicapoc®) already used in clinical trials on patients with sickle cell disease (SCD), is safe[152], and it is now property of a Pfizer spin out. Our data, could suggest to test KCa3.1 inhibitor in a combined treatment, for instance, with Riluzole[156,157], as a reinforced therapeutic strategy for human trials in ALS. In conclusion, our published data demonstrating that KCa3.1 is a good molecular target to reduce ALS-associated neuroinflammation and to protect MN from degeneration and future research perspectives will pave the road to design proof of concept experiments with high translational in the context of this fatal disease.

REFERENCES

1. Aran, F. A. Research on an as yet undescribed disease of the muscular system (progressive muscular atrophy). Arch. Gen. Med. 24, 15–35 (1848).
2. Cruveilhier, J. Sur la paralysiemusculaire, progressive, atrophique [French]. Bull. Acad. Med. (Paris) 18, 490–502, 546–583 (1852).
3. Charcot, J. M. &Joffroy, A. Deuxcas d'atrophiemusculaire progressive aveclesions de la substancegrise et desfaisceauxantero-lateraux de la moelleepiniere [French]. Arch. Physiol. Neurol. Pathol. 2, 744 (1869)
4. Leblond CS, Kaneb HM, Dion PA, Rouleau GA. Dissection of genetic factors associated with amyotrophic lateral sclerosis. Exp Neurol. 2014;262:91–101.
5. Cirulli, ET et al. Exome sequencing in amyotrophic lateral sclerosis identifies risk genes and pathways. Science, 347 (2015), pp. 1436-1441
6. Freischmidt, A., Müller, K., Zondler, L., Weydt, P., Mayer, B., Von Arnim, C. A., et al. (2015). Serum microRNAs in sporadic amyotrophic lateral sclerosis. Neurobiol. Aging36, e2615–e2620. doi: 10.1016/j.neurobiolaging.2015.06.00
7. Gurney, M. E. et al. Motor neuron degeneration in mice that express a human Cu,Zn superoxide dismutase mutation. Science 264, 1772–1775 (1994).
8. Phukan, J. et al. The syndrome of cognitive impairment in amyotrophic lateral sclerosis: a population-based study. J. Neurol. Neurosurg. Psychiatry 83, 102–108 (2012)
9. DeJesus-Hernandez, M. et al. Expanded GGGGCC hexanucleotide repeat in noncoding region of C9ORF72 causes chromosome 9p-linked FTD and ALS. Neuron 72, 245–256 (2011).
10. Logroscino, G. et al. Incidence of amyotrophic lateral sclerosis in Europe. J. Neurol. Neurosurg. Psychiatry 81, 385–390 (2010). This is one of the first studies to carry out a pooled analysis of six European population-based ALS registers and reports the incidence and clinical features of ALS in Europe. The design and the large number of patients with ALS involved in this study made it possible to compare the data collected in each country, unlike previous studies, and allowed the epidemiology of the disease to be accurately quantified.

11. Wittie M, Nelson LM, Usher S, Ward K, Benatar M. Utility of capture-recapture methodology to assess completeness of amyotrophic lateral sclerosis case ascertainment. Neuroepidemiology 2013; 40: 133–41.
12. O'Toole O, Traynor BJ, Brennan P, et al. Epidemiology and clinical features of amyotrophic lateral sclerosis in Ireland between 1995 and 2004. J NeurolNeurosurgPsychiatr 2008; 79: 30–32.
13. Huisman MHB, de Jong SW, van Doormaal PTC, et al. Population based epidemiology of amyotrophic lateral sclerosis using capture-recapture methodology. J NeurolNeurosurgPsychiatr 2011; 82: 1165–70.
14. DeJesus-Hernandez, M. et al. Expanded GGGGCC hexanucleotide repeat in noncoding region of C9ORF72 causes chromosome 9p-linked FTD and ALS. Neuron 72, 245–256 (2011).
15. Neumann, M. et al. Ubiquitinated TDP-43 in frontotemporal lobar degeneration and amyotrophic lateral sclerosis. Science 314, 130–133 (2006).
16. Rosen, D. R. et al. Mutations in Cu/Zn superoxide dismutase gene are associated with familial amyotrophic lateral sclerosis. Nature 362, 59–62 (1993).
17. Chiu, I. M. et al. A neurodegeneration- specific gene- expression signature of acutely isolated microglia from an amyotrophic lateral sclerosis mouse model. Cell Rep. 4, 385–401 (2013).
18. Wong, P. C. et al. An adverse property of a familial ALS-linked SOD1 mutation causes motor neuron disease characterized by vacuolar degeneration of mitochondria. Neuron 14, 1105–1116 (1995).
19. Bruijn, L. I. et al. Aggregation and motor neuron toxicity of an ALS-linked SOD1 mutant independent from wild-type SOD1. Science 281, 1851–1854 (1998). This study demonstrated that ALS-causing mutant SOD1 generates a toxicity that is independent of its dismutase activity.
20. Yamanaka, K. et al. Mutant SOD1 in cell types other than motor neurons and oligodendrocytes accelerates onset of disease in ALS mice. Proc. NatlAcad. Sci. USA 105, 7594–7599 (2008).
21. Ralph, G. S. et al. Silencing mutant SOD1 using RNAi protects against neurodegeneration and extends survival in an ALS model. Nature Med. 11, 429–433 (2005).
22. Yamanaka, K. et al. Astrocytes as determinants of disease progression in inherited amyotrophic lateral sclerosis. Nature Neurosci. 11, 251–253 (2008).

23. Boillee, S. et al. Onset and progression in inherited ALS determined by motor neurons and microglia. Science 312, 1389–1392 (2006). This report showed that the expression of mutant SOD1 in microglia accelerates the progression of ALS, establishing a role for non-cell autonomous events in motor neuron degeneration in the disease.
24. Pasquali, L., Lenzi, P., Biagioni, F., Siciliano, G. & Fornai, F. Cell to cell spreading of misfolded proteins as a therapeutic target in motor neuron disease. Curr. Med. Chem. 21, 3508–3534 (2014).
25. Conicella, A. E., Zerze, G. H., Mittal, J. & Fawzi, N. L. ALS mutations disrupt phase separation mediated by alpha-helical structure in the TDP-43 low-complexity C-terminal domain. Structure 24, 1537–1549 (2016).
26. Bergemalm, D. et al. Superoxide dismutase-1 and other proteins in inclusions from transgenic amyotrophic lateral sclerosis model mice. J. Neurochem. 114, 408–418 (2010).
27. Higgins, C. M., Jung, C. & Xu, Z. ALS-associated mutant SOD1G93A causes mitochondrial vacuolation by expansion of the intermembrane space and by involvement of SOD1 aggregation and peroxisomes. BMC Neurosci. 4, 16 (2003).
28. Corcia, P. et al. Molecular imaging of microglial activation in amyotrophic lateral sclerosis. PLoS ONE 7, e52941 (2012).
29. Brites, D. &Vaz, A. R. Microglia centered pathogenesis in ALS: insights in cell interconnectivity. Front. Cell Neurosci. 8, 117 (2014).
30. Wang, S. J., Wang, K. Y. & Wang, W. C. Mechanisms underlying the riluzole inhibition of glutamate release from rat cerebral cortex nerve terminals (synaptosomes). Neuroscience 125, 191–201 (2004).
31. Kretschmer, B. D., Kratzer, U. & Schmidt, W. J. Riluzole, a glutamate release inhibitor, and motor behavior. NaunynSchmiedebergs Arch. Pharmacol. 358, 181–190 (1998).
32. Smith, B. N. et al. Exome-wide rare variant analysis identifies TUBA4A mutations associated with familial ALS. Neuron 84, 324–331 (2014).
33. Brooks BR, Miller RG, Swash M, Munsat TL, World Federation of Neurology Research Group on Motor Neuron Diseases. El Escorial revisited: revised criteria for the diagnosis of amyotrophic lateral sclerosis. AmyotrophLateralScler Other Motor NeuronDisord 2000: 293–99.

34. Geevasinga N, Menon P, Scherman DB, et al. Diagnostic criteria in amyotrophic lateral sclerosis: a multicenter prospective study. Neurology 2016; 87: 684–90.
35. Byrne, S. et al. Proposed criteria for familial amyotrophic lateral sclerosis. Amyotroph. LateralScler. 12, 157–159 (2011).
36. Vajda, A. et al. Genetic testing in ALS: a survey of current practices. Neurology 88, 991–999 (2017).
37. Gaiani, A. et al. Diagnostic and prognostic biomarkers in amyotrophic lateral sclerosis: neurofilament light chain levels in definite subtypes of disease. JAMA Neurol. 74, 525–532 (2017).
38. Elamin, M. et al. Predicting prognosis in amyotrophic lateral sclerosis: a simple algorithm. J. Neurol. 262, 1447–1454 (2015).
39. Pinto, S. & de Carvalho, M. Correlation between Forced Vital Capacity and Slow Vital Capacity for the assessment of respiratory involvement in amyotrophic lateral sclerosis: a prospective study. Amyotroph. LateralScler. FrontotemporalDegener. 18, 86–91 (2017).
40. Morgan, R. K. et al. Use of Sniff nasal-inspiratory force to predict survival in amyotrophic lateral sclerosis. Am. J. Respir. Crit. Care Med. 171, 269–274 (2005).
41. Iyer, P. M. et al. Functional connectivity changes in resting-state EEG as potential biomarker for amyotrophic lateral sclerosis. PLoS ONE 10, e0128682 (2015).
42. Canosa, A. et al. 18F-FDG-PET correlates of cognitive impairment in ALS. Neurology 86, 44–49 (2016).
43. Reich-Slotky R, Andrews J, Cheng B, et al. Body mass index (BMI) as predictor of ALSFRS-R score decline in ALS patients. Amyotroph Lateral Scler Frontotemporal Degener 2013; 14: 212–16.
44. Stavroulakis T, Baird WO, Baxter SK, Walsh T, Shaw PJ, McDermott CJ. The impact of gastrostomy in motor neurone disease: challenges and benefits from a patient and carer perspective. BMJ Support Palliat Care 2016; 6: 52–59.
45. Bourke SC, Tomlinson M, Williams TL, Bullock RE, Shaw PJ, Gibson GJ. Effects of non-invasive ventilation on survival and quality of life in patients with amyotrophic lateral sclerosis: a randomised controlled trial. Lancet Neurology 2006; 5: 140–47.
46. National Clinical Guideline Centre (UK). Motor neurone disease: assessment and management. London: National Institute for Health and Care Excellence, 2016.

47. Lacomblez, L., Bensimon, G., Leigh, P. N., Guillet, P. & Meininger, V. Dose-ranging study of riluzole in amyotrophic lateral sclerosis. Amyotrophic Lateral Sclerosis/Riluzole Study Group II. Lancet 347, 1425–1431 (1996). Based on the landmark trial of riluzole in patients with ALS in 1994, this study presents an assessment of the efficacy of the drug at different doses in a double-blind, placebo-controlled, multicentre trial, identifying that the 100 mg dose of riluzole had the best benefit-to-risk ratio; this is the recommended dose used to treat the symptoms of ALS today.
48. Dyer, A. M. & Smith, A. Riluzole 5 mg / mL oral suspension: for optimized drug delivery in amyotrophic lateral sclerosis. DrugDes. DevelTher. 11, 59–64 (2017).
49. Writing Group, Edaravone (MCl-186) ALS 19 Study Group. Safety and efficacy of edaravone in well defined patients with amyotrophic lateral sclerosis: a randomised, double-blind, placebo-controlled trial. Lancet Neurol. 16, 505–512 (2017).
50. Hardiman, O. & van den Berg, L. H. Edaravone: a new treatment for ALS on the horizon? Lancet Neurol. 16, 490–491 (2017).
51. Miller TM, Pestronk A, David W, et al. An antisense oligonucleotide against SOD1 delivered intrathecally for patients with SOD1 familial amyotrophic lateral sclerosis: a phase 1, randomised, first-in-man study. Lancet Neurol 2013; 12: 435–42.
52. Lagier-Tourenne, C. et al. Targeted degradation of sense and antisense C9orf72 RNA foci as therapy for ALS and frontotemporal degeneration. Proc. NatlAcad. Sci. USA 110, E4530–E4539 (2013).
53. RíoHortega, P. Noticia de un nuevo y fácilmétodo para la coloración de la neuroglia y eltejidoconjuntivo. Trab. Lab. Invest. Biol. 15, 367–378 (1918).
54. Alliot, F., Godin, I. & Pessac, B. Microglia derive from progenitors, originating from the yolk sac, and which proliferate in the brain. Brain Res. Dev. Brain Res. 117, 145–152 (1999).
55. Ginhoux, F. et al. Fate mapping analysis reveals that adult microglia derive from primitive macrophages. Science 330, 841–845 (2010).
56. Van Furth, R. & Cohn, Z. A. The origin and kinetics of mononuclear phagocytes. J. Exp. Med. 128, 415–435 (1968).
57. Bruttger, J. et al. Genetic cell ablation reveals clusters of local self- renewing microglia in the mammalian central nervous system. Immunity 43, 92–106 (2015).
58. Tay, T. L. et al. A new fate mapping system reveals context- dependent random or clonal expansion of microglia. Nat. Neurosci. 20, 793–803 (2017).

59. Askew, K. et al. Coupled proliferation and apoptosis maintain the rapid turnover of microglia in the adult brain. Cell Rep. 18, 391–405 (2017).
60. Reu, P. et al. The lifespan and turnover of microglia in the human brain. Cell Rep. 20, 779–784 (2017).
61. Huang, Y. et al. Repopulated microglia are solely derived from the proliferation of residual microglia after acute depletion. Nat. Neurosci. 21, 530–540 (2018).
62. Ransohoff, R. M. & El Khoury, J. Microglia in health and disease. Cold Spring Harb. Perspect. Biol. 8, a020560 (2015).
63. Hickman, S. E. et al. The microglial sensome revealed by direct RNA sequencing. Nat. Neurosci. 16, 1896–1905 (2013).
64. Kaur, C., Hao, A. J., Wu, C. H. & Ling, E. A. Origin of microglia. Microsc. Res. Tech. 54, 2–9 (2001).
65. Davalos, D. et al. ATP mediates rapid microglial response to local brain injury in vivo. Nat. Neurosci. 8, 752–758 (2005).
66. Nimmerjahn, A., Kirchhoff, F. &Helmchen, F. Resting microglial cells are highly dynamic surveillants of brain parenchyma in vivo. Science 308, 1314–1318 (2005)
67. Tremblay, M. E., Lowery, R. L. & Majewska, A. K. Microglial interactions with synapses are modulated by visual experience. PLoSBiol. 8, e1000527 (2010).
68. Wake, H., Moorhouse, A. J., Jinno, S., Kohsaka, S. &Nabekura, J. Resting microglia directly monitor the functional state of synapses in vivo and determine the fate of ischemic terminals. J. Neurosci. 29, 3974–3980 (2009).
69. Schafer, D. P. & Stevens, B. Phagocytic glial cells: sculpting synaptic circuits in the developing nervous system. Curr. Opin. Neurobiol. 23, 1034–1040 (2013).
70. Paolicelli, R. C. et al. Synaptic pruning by microglia is necessary for normal brain development. Science 333, 1456–1458 (2011).
71. Kettenmann, H., Kirchhoff, F. &Verkhratsky, A. Microglia: new roles for the synaptic stripper. Neuron 77, 10–18 (2013).
72. Parkhurst, C. N. et al. Microglia promote learning- dependent synapse formation through brain- derived neurotrophic factor. Cell 155, 1596–1609 (2013).
73. Butovsky, O. et al. Modulating inflammatory monocytes with a unique microRNA gene signature ameliorates murine ALS. J. Clin. Invest. 122, 3063–3087 (2012).
74. Sierra, A. et al. Microglia shape adult hippocampal neurogenesis through apoptosis-coupled phagocytosis. Cell Stem Cell 7, 483–495 (2010).

75. Ransohoff, R. M. & Cardona, A. E. The myeloid cells of the central nervous system parenchyma. Nature 468, 253–262 (2010).
76. Kettenmann, H., Hanisch, U. K., Noda, M. &Verkhratsky, A. Physiology of microglia. Physiol. Rev. 91, 461–553 (2011).
77. Hanisch, U. K. &Kettenmann, H. Microglia: active sensor and versatile effector cells in the normal and pathologic brain. Nat. Neurosci. 10, 1387–1394 (2007).
78. Hanisch, U. K. Functional diversity of microglia - how heterogeneous are they to begin with? Front. Cell. Neurosci. 7, 65 (2013).
79. Mantovani, A., Sica, A. &Locati, M. Macrophage polarization comes of age. Immunity 23, 344–346 (2005). 24. Martinez, F. O. & Gordon, S. The M1 and M2 paradigm of macrophage activation: time for reassessment. F1000Prime Rep. 6, 13 (2014).
80. Martinez, F. O. & Gordon, S. The M1 and M2 paradigm of macrophage activation: time for reassessment. F1000Prime Rep. 6, 13 (2014).
81. Ransohoff, R. M. A polarizing question: do M1 and M2 microglia exist? Nat. Neurosci. 19, 987–991 (2016).
82. Meeuwsen S, Bsibsi M, Persoon-Deen C, Ravid R, van Noort JM. Cultured human adult microglia from different donors display stable cytokine, chemokine and growth factor gene profiles but respond differently to a pro-inflammatory stimulus. Neuroimmunomodulation (2005); 12:235–245.
83. Sierra A, Gottfried-Blackmore AC, McEwen BS, Bulloch K. Microglia derived from aging mice exhibit an altered inflammatory profile. Glia (2007); 55:412–424.
84. Hristova M, Cuthill D, Zbarsky V, Acosta-Saltos A, Wallace A, Blight K, Buckley SM, Peebles D, Heuer H, Waddington SN, Raivich G. Activation and deactivation of periventricular white matter phagocytes during postnatal mouse development. Glia (2010); 58: 11–28.
85. Henkel, J. S. et al. Presence of dendritic cells, MCP-1, and activated microglia/macrophages in amyotrophic lateral sclerosis spinal cord tissue. Ann. Neurol. 55, 221–235 (2004).
86. Turner, M. R. et al. Evidence of widespread cerebral microglial activation in amyotrophic lateral sclerosis: an [11C](R)-PK11195 positron emission tomography study. Neurobiol. Dis. 15, 601–609 (2004).

87. Al-Chalabi, A., van den Berg, L. H. &Veldink, J. Gene discovery in amyotrophic lateral sclerosis: implications for clinical management. Nat. Rev. Neurol. 13, 96–104 (2017).
88. Li, Y. R., King, O. D., Shorter, J., and Gitler, A. D. (2013). Stress granules as crucibles of ALS pathogenesis. J. Cell Biol. 201, 361–372. doi: 10.1083/jcb. 201302044
89. Ogawa, M., and Furukawa, Y. (2014). A seeded propagation of Cu, Zn-superoxide dismutase aggregates in amyotrophic lateral sclerosis. Front. Cell. Neurosci. 8:83. doi: 10.3389/fncel.2014.00083
90. Liao, B., Zhao, W., Beers, D. R., Henkel, J. S., and Appel, S. H. (2012). Transformation from a neuroprotective to a neurotoxic microglial phenotype in a mouse model of ALS. Exp. Neurol. 237, 147–152. doi: 10.1016/j.expneurol.2012. 06.011
91. Hall, E. D., Oostveen, J. A. & Gurney, M. E. Relationship of microglial and astrocytic activation to disease onset and progression in a transgenic model of familial ALS. Glia 23, 249–256 (1998).
92. Yamanaka, K. et al. Mutant SOD1 in cell types other than motor neurons and oligodendrocytes accelerates onset of disease in ALS mice. Proc. Natl. Acad. Sci. USA 105, 7594–7599 (2008).
93. Apolloni, S., Amadio, S., Montilli, C., Volonté, C. &D'Ambrosi, N. Ablation of P2X7 receptor exacerbates gliosis and motoneuron death in the SOD1-G93A mouse model of amyotrophic lateral sclerosis. Hum. Mol. Genet. 22, 4102–4116 (2013).
94. Liao, B., Zhao, W., Beers, D. R., Henkel, J. S. & Appel, S. H. Transformation from a neuroprotective to a neurotoxic microglial phenotype in a mouse model of ALS. Exp. Neurol. 237, 147–152 (2012).
95. Lewis,C.A.,et al., (2012). The neuroinflammatory response in ALS: the roles of microglia and T cells. Neurol. Res. Int. 2012,803701. doi: 10.1155/2012/803701
96. Gerber,Y.N.,Sabourin,J.C.,Rabano,M.,Vivanco,M.,andPerrin,F.E.(2012).Early functional deficit and microglial disturbances in a mouse model of amyotrophic lateral sclerosis. PLoS ONE 7:e36000. doi: 10.1371/journal.pone.0036000
97. Frakes, A. E. et al. Microglia induce motor neuron death via the classical NF-κ B pathway in amyotrophic lateral sclerosis. Neuron 81, 1009–1023 (2014).

98. Meissner, F., Molawi, K. &Zychlinsky, A. Mutant superoxide dismutase 1-induced IL-1beta accelerates ALS pathogenesis. Proc. Natl. Acad. Sci. USA 107, 13046–13050 (2010).
99. O'Connell, R. M. et al. MicroRNA-155 promotes autoimmune inflammation by enhancing inflammatory T cell development. Immunity 33, 607–619 (2010).
100. O'Rourke, J. G. et al. C9orf72 BAC transgenic mice display typical pathologic features of ALS/FTD. Neuron 88, 892–901 (2015).
101. O'Rourke, J. G. et al. C9orf72 is required for proper macrophage and microglial function in mice. Science 351, 1324–1329 (2016).
102. Spiller, K. J. et al. Microglia-mediated recovery from ALS-relevant motor neuron degeneration in a mouse model of TDP-43 proteinopathy. Nat. Neurosci. 21, 329–340 (2018).
103. Paolicelli, R. C. et al. TDP-43 depletion in microglia promotes amyloid clearance but also induces synapse loss. Neuron 95, 297–308.e6 (2017).
104. Kunzelmann K. Ion channels and cancer. J MembrBiol (2005); 205:159-173.
105. Arcangeli A, Crociani O, Lastraioli E, Masi A, Pillozzi S, Becchetti A. Targeting ion channels in cancer: a novelfrontier in antineoplastic therapy. CurrMedChem (2009); 16(1):66-93.
106. Cuddapah VA, Sontheimer H. Ion channels and transporters in cancer. 2. Ion channels and the control of cancer cell migration. Am J Physiol (2011); 301(3): C541-C549.
107. Ritchie MF, Zhou Y, Soboloff J. WT1/EGR1 mediated control of STIM1 expression and function in cancer cells. Front Biosci (2011); 16:2402-2415.
108. Ding X, He Z, Zhou K, Cheng J, Yao H, Lu D, Cai R, Jin Y, Dong B, Xu Y, Wang Y. Essential role of TRPC6 channels in G2/M phase transition and development of human glioma. J Natl Cancer Inst (2010); 102(14):1052-1068.
109. Cuddapah VA, Habela CW, Watkins S, Moore LS, Barclay TT, Sontheimer H. Kinase activation of ClC-3 accelerates cytoplasmic condensation during mitotic cell rounding. Am J Physiol (2012); 302(3): C527-C538.
110. Giannone G, Ronde P, Gaire M, Haiech J, Takeda K. Calcium oscillations trigger focal adhesion disassembly in human U87 astrocytoma cells. J Biol Chem (2002); 277(29):26364-26371.

111. Reetz G, Reiser G. $[Ca^{2+}]_i$oscillations induced by bradykinin in rat glioma cells associated with Ca^{2+}storedependent Ca^{2+} influx are controlled by cell volume and by membrane potential. Cell Calcium (1996); 19(2):143-156.
112. Berkefeld H, Fakler B, Schulte U. Ca^{2+}-activated K^+ channels: from protein complexes to function. Physiol Rev (2010); 90(4): 1437-1459.
113. Wei AD, Gutman GA, Aldrich R, Chandy KG, Grissmer S, Wulff H. International Union of Pharmacology. LII. Nomenclature and molecular relationships of calcium-activated potassium channels. Pharmacol Rev (2005); 57(4):463-472.
114. Logsdon NJ, Kang J, Togo JA, Christian EP, Aiyar J. A novel gene, hKCa4, encodes the calcium-activated potassium channel in human T lymphocytes. J Biol Chem (1997); 272(52):32723-32726.
115. Ishii TM, Silvia C, Hirschberg B, Bond CT, Adelman JP, Maylie J. A human intermediate conductance calcium-activated potassium channel. Proc Natl Acad Sci USA (1997); 94(21):11651-11656.
116. Xia XM, Fakler B, Rivard A, Wayman G, Johnson-Pais T, Keen JE, Ishii T, Hirschberg B, Bond CT, Lutsenko S, Maylie J, Adelman JP. Mechanism of calcium gating in small-conductance calcium-activated potassium channels. Nature (1998); 395(6701):503-507.
117. Cheong A, Bingham AJ, Li J, Kumar B, Sukumar P, Munsch C, Buckley NJ, Neylon CB, Porter KE, Beech DJ, Wood IC. Downregulated REST transcription factor is a switch enabling critical potassium channel expression and cell proliferation. Mol Cell (2005); 20(1): 45-52.
118. Ghanshani S, Wulff H, Miller MJ, Rohm H, Neben A, Gutman GA, Cahalan MD, Chandy KG. Up-regulation of the IKCa1 potassium channel during Tcell activation: Molecular mechanism and functional consequences. J Biol Chem (2000); 275(47):37137-37149
119. Gerlach AC, Gangopadhyay NN, Devor DC. Kinase-dependent regulation of the intermediate conductance, calcium-dependent potassium channel, hIK1. J Biol Chem (2000); 275(1):585-598.
120. Srivastava S, Li Z, Ko K, Choudhury P, Albaqumi M, Johnson AK, Yan Y, Backer JM, Unutmaz D, Coetzee WA, Skolnik EY. Histidine phosphorylation of the potassium channel KCa3.1 by nucleoside diphosphate kinase B is required for activation of KCa3.1 and CD4 T cells. Mol Cell (2006); 24(5):665-675.

121. Wulff H, Castle NA. Therapeutic potential of KCa3.1 blockers: recent advances and promising trends. Expert Rev Clin Pharmacol (2010); 3(3):385-396.
122. Tharp DL, Wamhoff BR, Wulff H, Raman G, Cheong A, Bowles DK. Local delivery of the KCa3.1 blocker, TRAM-34, prevents acute angioplasty-induced coronary smooth muscle phenotypic modulation and limits stenosis. ArteriosclerThrombVasc Bio (2008); 28(6):1084-1089.
123. Toyama K, Wulff H, Chandy KG, Azam P, Raman G, Saito T, Fujiwara Y, Mattson DL, Das S, Melvin JE, Pratt PF, Hatoum OA, Gutterman DD, Harder DR, Miura H. The intermediate-conductance calcium-activated potassium channel KCa3.1 contributes to atherogenesis in mice and humans. J Clin Invest (2008); 118(9):3025-3037.
124. Reich EP, Cui L, Yang L, Pugliese-Sivo C, Golovko A, Petro M, Vassileva G, Chu I, Nomeir AA, Zhang LK, Liang X, Kozlowski JA, Narula SK, Zavodny PJ, Chou CC. Blocking ion channel KCNN4 alleviates the symptoms of experimental autoimmune encephalomyelitis in mice. Eur J Immunol (2005); 35(4):1027-1036.
125. Chen J, Yao Y, Gong C, Yu F, Su S, Chen J, Liu B, Deng H, Wang F, Lin L, Yao H, Su F, Anderson KS, Liu Q, Ewen ME, Yao X, Song E. CCL18 from tumor-associated macrophages promotes breast cancer metastasis via PITPNM3. Cancer Cell. (2011); 19(4):541–555.
126. Lam J, Wulff H. The Lymphocyte Potassium Channels Kv1.3 and KCa3.1 as Targets for immunosuppression. Drug Dev Res. (2011); 72(7):573-584.
127. Higashimori H, Sontheimer H. Role of Kir4.1 channels in growth control of glia. Glia (2007); 55(16):1668-1679.
128. Watkins S, Sontheimer H. Hydrodynamic cellular volume changes enable glioma cell invasion. J Neurosci (2011); 31(47):17250-17259.
129. Habela CW, Sontheimer H. Cytoplasmic volume condensation is an integral part of mitosis. Cell Cycle (2007); 6(13):1613-1620.
130. Habela CW, Ernest NJ, Swindall AF, Sontheimer H. Chloride accumulation drives volume dynamics underlying cell proliferation and migration. J Neurophysiol (2009); 101(2):750-757.
131. Habela CW, Olsen ML, Sontheimer H. ClC3 is a critical regulator of the cell cycle in normal and malignant glial cells. J Neurosci (2008); 28(37):9205-9217.
132. Weaver AK, Bomben VC, Sontheimer H. Expression and function of calcium-activated potassium channels in human glioma cells. Glia (2006); 54(3):223-233.

133. McCoy E, Sontheimer H. Expression and function of water channels (aquaporins) in migrating malignant astrocytes. Glia (2007); 55:1034-1043.
134. Montana V, Sontheimer H. Bradykinin promotes the chemotactic invasion of primary brain tumors. J Neurosci (2011); 31:4858-4867.
135. Bomben VC, Sontheimer H. Disruption of transient receptor potential canonical channel 1 causes incomplete cytokinesis and slows the growth of human malignant gliomas. Glia (2010); 58(10):1145-1156.
136. Haas BR, Sontheimer H. Inhibition of the sodiumpotassium- chloride cotransporter isoform-1 reduces glioma invasion. Cancer Res (2010); 70(13):5597-5606.
137. Cuddapah VA, Sontheimer H. Molecular interaction and functional regulation of ClC-3 by Ca2+/calmodulin-dependent protein kinase II (CaMKII) in human malignant glioma. J Biol Chem (2010); 285(15): 11188-11196.
138. Mamelak AN, Rosenfeld S, Bucholz R, Raubitschek A, Nabors LB, Fiveash JB, Shen S, Khazaeli MB, Colcher D, Liu A, Osman M, Guthrie B, Schade-Bijur S, Hablitz DM, Alvarez VL, Gonda MA. Phase I single-dose study of intracavitaryadministered iodine-131-TM-601 in adults with recurrent high-grade glioma. J ClinOncol (2006); 24(22):3644-3650.
139. Haas BR, Cuddapah VA, Watkins S, Rohn KJ, Dy TE, Sontheimer H. With-No-Lysine Kinase 3 (WNK3) stimulates glioma invasion by regulating cell volume. Am J Physiol Cell Physiol (2011); 301(5):C1150-C1160.
140. Kaushal V, Koeberle PD, Wang Y, Schlichter LC. The Ca^{2+}-activated K^{+} channel KCNN4/KCa3.1 contributes to microglia activation and nitric oxide-dependent neurodegeneration. J Neurosci. (2007); 27(1):234-44.
141. Maezawa I, Jenkins DP, Jin BE, Wulff H. Microglial KCa3.1 Channels as a Potential Therapeutic Target for Alzheimer's Disease. Int J Alzheimers Dis. (2012); 2012:868972.
142. Ferreira R, Lively S, Schlichter LC. IL-4 type 1 receptor signaling up-regulates KCNN4 expression, and increases the KCa3.1 current and its contribution to migration of alternative-activated microglia. Front Cell Neurosci. (2014);8:183. doi: 10.3389/fncel.2014.00183.
143. D'Alessandro, M Catalano, M Sciaccaluga, G Chece, R Cipriani, M Rosito, A Grimaldi, C Lauro, G Cantore, A Santoro,B Fioretti, F Franciolini, H Wulff and C Limatola. KCa3.1 channels are involved in the infiltrative behavior of glioblastoma in vivo. Cell Death and Disease (2013); 4, e773; doi:10.1038/cddis.2013.279

144. Eder C, Heinemann U. Potassium currents in acutely isolated neurons from superficial and deep layers of the juvenile rat entorhinal cortex. Pflugers Arch. (1996); 432(4):637-43.
145. Grimaldi A, D'Alessandro G, Golia MT, Grössinger EM, Di Angelantonio S, Ragozzino D, Santoro A, Esposito V, Wulff H, Catalano M, Limatola C. KCa3.1 inhibitionswitches the phenotype of glioma infiltrating microglia/macrophages. Cell Death and Dis. 2016;7:e2174.
146. H. Wulff, M. J. Miller, W. Hänsel, S. Grissmer, M. D. Cahalan, and K. G. Chandy, "Design of a potent and selective inhibitor of the intermediate- conductance Ca2+-activated K+ channel, IKCa1: a potential immunosuppressant," Proceedings of the National Academy of Sciences of the United States of America, vol. 97, no. 14, pp. 8151–8156, 2000.
147. T. Begenisich, T. Nakamoto, C. E. Ovitt et al., "Physiological roles of the intermediate conductance, Ca2+- activated potassium channel Kcnn4," The Journal Biological Chemistry, vol. 279, no. 46, pp. 47681–47687, 2004.
148. H. Si, W. T. Heyken, S. E. Wolfle et al., "Impaired ¨ endothelium-derived hyperpolarizing factor-mediated dilations and increased blood pressure in mice deficient of the intermediate-conductance Ca2+-activated K+ channel," Circulation Research, vol. 99, no. 5, pp. 537–544, 2006.
149. I. Grgic, B. P. Kaistha, S. Paschen et al., "Disruption of the Gardos channel (KCa3.1) in mice causes subtle erythrocyte macrocytosis and progressive splenomegaly," PflugersArchiv European Journal of Physiology, vol. 458, no. 2, pp. 291–302, 2009.
150. Y. J. Chen, G. Raman, S. Bodendiek, M. E. O'Donnell, and H. Wulff, "The KCa3.1 blocker TRAM-34 reduces infarction and neurological deficit in a rat model of ischemia/reperfusion stroke," Journal of Cerebral Blood Flow and Metabolism, vol. 31, no. 12, pp. 2363–2374, 2011.
151. K. I. Ataga, E. P. Orringer, L. Styles et al., "Dose-escalation study of ICA-17043 in patients with sickle cell disease," Pharmacotherapy, vol. 26, no. 11, pp. 1557–1564, 2006.
152. Ataga K.I., Reid M., Ballas S.K., Yasin Z., Bigelow C., James L.S., Smith W.R., Galacteros F., Kutlar A., Hull J.H., Stocker J.W., 2011. Study Investigators. Improvements in haemolysis and indicators of erythrocyte survival do not correlate with acute vaso-occlusive crises in patients with sickle cell disease: a phase III

randomized, placebo-controlled, double-blind study of the Gardos channel blocker senicapoc (ICA-17043). Br J Haematol 153, 92–104.

153. Gordon PH et al. (2007) Efficacy of minocycline in patients with amyotrophic lateral sclerosis: a phase III randomised trial. Lancet Neurol6: 1045–1053.
154. Feske S., Wulff H., Skolnik EY., 2015. Ion channels in innate and adaptive immunity. Annu. Rev. Immunol. 33, 291-353.
155. Zierler S., Sumoza-Toledo A., Suzuki S., Dúill F.Ó., Ryazanova L.V., Penner R., Ryazanov A.G., Fleig A. 2016. TRPM7 kinase activity regulates murine mast cell degranulation J Physiol 594(11), 2957-70.
156. Miller RG et al (2012) Riluzole for amyotrophic lateral sclerosis (ALS)/motor neuron disease (MND). Cochrane Database Syst Rev. 2012 Mar 14;(3):CD001447. doi: 10.1002/14651858.CD001447.pub3.
157. Gurney ME, Cutting FB, Zhai P, et al. Benefit of vitamin E, riluzole, and gabapentin in a transgenic model of familial amyotrophic lateral sclerosis. Ann Neurol. 1996;39(2):147-157.